UNIVERSITY OF HELSINKI
DIVISION OF GEOPHYSICS

REPORT SERIES IN GEOPHYSICS

No 45

Cover: The visible light satellite image covering the area where the data has been collected for this study. The instrument is MODIS onboard Terra satellite (© NASA).

INHERENT AND APPARENT OPTICAL PROPERTIES IN RELATION TO WATER QUALITY IN NORDIC WATERS

Antti Herlevi

University of Helsinki, Division of Geophysics, Helsinki, Finland

HELSINKI 2002

ISBN 952-10-0871-7
ISSN 0355-8630

Helsinki 2002
Yliopistopaino

Report Series in Geophysics No. 45
ISBN 952-10-0871-7 (paperback)
ISBN 952-10-0872-5 (PDF)

INHERENT AND APPARENT OPTICAL PROPERTIES

IN RELATION TO

WATER QUALITY

IN

NORDIC WATERS

Antti Herlevi

Academic dissertation in Geophysics, to be presented, with the permission of the Faculty of Science of the University of Helsinki, for public criticism in the Auditorium XII of the main building, Unioninkatu 34, Helsinki, on December 20th, 2002, at 12 o'clock.

Helsinki 2002

"*Let there be light,*"

and there was light. God saw that the light was good.

"*Let the water under the sky be gathered into one place,*"

and the gathered waters he called "seas". And God saw that it was good.

- the beginning of aquatic optics (*Gen 1:3-4,9-10*)

Contents

This thesis is based on the following articles, referred to in the text by Roman numerals:

I. Arst, H., A. Erm, K. Kallaste, S. Mäekivi, A. Reinart, A. Herlevi, P. Noges and T. Noges, 1999. Investigation of Estonian and Finnish lakes by optical measurements in 1992-1997. *Proc. Estonian Acad. Sci. Biol. Ecol.*, **48**, 1, 5-24.

II. Arst, H., S. Mäekivi, T. Lukk and A. Herlevi, 1997. Calculating irradiance penetration into water bodies from the measured beam attenuation coefficient. *Limnology and Oceanography*, 42(2), 1997, 379-385.

III. Arst, H., A. Erm, A. Reinart, L. Sipelgas and A. Herlevi, 2002. Calculating Irradiance Penetration into Water Bodies from the Measured Beam Attenuation Coefficient II : Application of the Improved Model to Different Types of Lakes. *Nordic Hydrology*, 33 2/3, 2002, 227-240.

IV. Herlevi, A., H. Virta, H. Arst and A. Erm, 1999. Results of light absorption/attenuation measurements in Finnish and Estonian lakes in summer 1997. *Proc. Estonian Acad. Sci. Biol. Ecol.*, **48**, 1, 46-62.

V. Reinart A. and A. Herlevi, 1999. Diffuse attenuation coefficient in some Estonian and Finnish lakes. *Proc. Estonian Acad. Sci. Biol. Ecol.*, **48**, 4, 267-283.

VI. Kutser, T., A. Herlevi, K. Kallio, H. Arst, 2001. A hyperspectral model for interpretation of passive optical remote sensing data from turbid lakes. *The Science of the Total Environment*, 268 (1-3) (2001) pp. 47-58.

VII. Herlevi, A., 2002. Relations between inherent and apparent optical properties in Finnish and Estonian lakes. Submitted and revised for *Nordic Hydrology*.

VIII. Herlevi, A., 2002. A Study of Scattering, Backscattering and a Hyperspectral Reflectance Model for Boreal Waters. *Geophysica* (2002), 38(1-2), 113-132

Report Series in Geophysics No. 45

Inherent and Apparent Optical Properties in Relation to Water Quality in Nordic Waters

Antti Herlevi

Division of Geophysics
Department of Physical Sciences
P.O. Box 64
FIN-00014 University of Helsinki
Finland

Abstract

Aquatic optics is concerned with the behavior of light in aquatic media studying optical properties of the natural aquatic environment and underwater solar radiation field. It has up to recent years been mainly oceanographic in its orientation. This study did not separate it in a traditional way (into oceanographic and limnetic), but was concentrated on turbid and semi turbid multicomponental coastal waters and lakes.

The following facts motivated this work: there has been an essential shortage of field results and valid optical models for multicomponent waters. In these waters different types of dissolved and suspended matter occur often in great concentrations, thus they are challenging investigation objects. The thousands of lakes and coastal areas in Nordic countries that can be studied by optical methods are important for the economy and recreation.

This study summarizes the author's work in aquatic optics. It is the first extensive work in Finland concentrating on spectral characteristics of optical properties, their mutual relations and hyperspectral modelling in relation to water quality as well as the variability in optical properties in Nordic waters. It provides new information on the optics of boreal waters, about the relationships between inherent and apparent optical properties, as well as spectral characteristics and variations in scattering and backscattering. These are important for optical models and remote sensing of lakes and coastal waters. It is also valuable in providing some practical tools and understanding for research and monitoring of water quality. A large database from years 1994-2001 of optical properties and bio-optical parameters from Nordic waters was collected, processed and analyzed during this study.

Looking at the whole data set it was concluded that the variation in the optical properties is large both temporally and spatially.

A model connecting beam attenuation coefficient, c and diffuse attenuation coefficient, K_d was developed using formulae connecting the values of K_d, absorption coefficient, a and the scattering coefficient, b for different illumination conditions. Correlation analysis of the model's results between the measured and calculated K_d gave the relationship $K_{dm} = 1.0023\ K_{dc}$, with a statistically significant correlation coefficient 0.961.

The relationships between an apparent optical property K_d and two inherent optical properties absorption, a and scattering, b were studied. Two separate tests were used. The results deviated from the earlier results found by other authors. The difference was considerable (about 100 %), especially in case of brown waters in the coefficient connected with scattering. One explanation given was the type of the boreal waters (brownish, but still include substantial amounts of scattering material).

The spectral distribution of the total scattering, b obtained from the ac-9 absorption/attenuation meter data was investigated. Generally (by other authors) there seems to be evidence that b varies approximately with λ^{-1}. Our results showed that the exponent of the wavelength varied between 0.13 and 2.42, the mean value being 0.78. It was also clearly larger in May/June (n_b=0.90) than in August (n_b=0.66). This could be explained by the size and type of the particles in the water. There was also in general a poor correlation between the average scattering coefficient b and the spectral wavelength dependency, except in spring (R^2=0.78 in May). However, when the correlation was good, it was positive. This was contradictory to the general results found by other authors. If one intends to find a spectrum for total scattering, the time of the year is crucial and also the type of water, but as rule of thumb b varies approximately with $\lambda^{-0.8}$ (or λ^{-1}).

The backscattering probability, $\tilde{b}_b=b_b/b$, and the coefficient C in an equation relating reflectance to backscattering and absorption were studied. The value of C was found to be changing with the water type as well as with the solar elevation and it was slightly smaller than the value proposed by *Kirk* (1984). The results of the backscattering probability study show that $\tilde{b}_b$ is growing with turbidity except in the very turbid lakes in a similar fashion with C. The size distribution and the type of scattering particles were found to be crucial for the behavior of $\tilde{b}_b$ as well. Moving from brown waters towards more turbid waters backscattering increases due to the increase in the amount of inorganic particles, except in very turbid cases where chlorophyll and organic particles dominate the scattering process. The average calculated value of $\tilde{b}_b$ was found to be 0.015. Our results indicate that even the 'clear' Nordic lakes contain relatively much chlorophyll to diminish the backscattering probability or the value of C. The average values for $\tilde{b}_b$ obtained from direct measurements in Sweden were found to be 0.014 in varying waters and 0.019 in lake Vänern. The wavelength dependence (n_B) of $\tilde{b}_b$ was also studied. The average value for n_B (in λ^{-nB}) was found to be 0.63 and it was larger in spring than in autumn.

Lastly a hyperspectral model was described. It was developed to test the possibility of estimating chlorophyll-a, dissolved and total organic carbon and suspended matter concentrations from the remotely measured diffuse reflectance in Nordic waters. The database for the last version of the model was collected during 1997-2001 (paper VIII). The forward model tested in paper VIII worked quite well, without favoring any particular water type. The inverse mode of the model (in paper VI) worked also well, but underestimated chlorophyll-a concentrations in the water. The correlation between measured and estimated values (R^2=0.80) is acceptable, but the relative errors in chlorophyll estimations are high, especially in case of small concentrations. Absorption by yellow substance could be relatively well estimated as well as the concentrations of non-chlorophyllous particles (C_{SM}), but the model underestimates C_{SM} values.

The relations between the inherent and apparent optical properties, studied in this work, are interesting from a purely physical point of view, but they have a considerable practical importance too. There are a number of practical possibilities to use these relationships described in the chapters 7.2. and 7.3.. There maybe many reasons why one or several parameters can not be measured and these relations can be used to obtain representative values to replace the missing data.

We can use a hyperspectral model to deduce concentrations of optically active substances (OAS) from remote sensing reflectance. The model can be used to monitor water quality rapidly in large areas using satellite or airborne remote sensing. In addition, if a simple model is available, water quality parameters may be obtained using a portable spectrometer measuring reflectance above water on a moving boat. This is important in our small lakes and archipelago where satellite data is not usable. This kind of system could also be used in point measurements following temporal variations.

Key words: apparent and inherent optical properties, water quality, optically active substances, scattering, backscattering, remote sensing, bio-optical modeling, Boreal waters

1 Introduction

1.1 Optical research and monitoring

Optics is that part of physics that deals with light. The behavior of light is greatly affected by the nature of the medium through which it is passing. Aquatic optics is concerned with the behavior of light in aquatic media. It can be subdivided into limnetic and oceanographic optics according to whether fresh or salty waters are under consideration. Aquatic optics has up to recent years been mainly oceanographic in its orientation. This study does not separate them in a traditional way, but is concentrated on turbid and semi turbid multicomponental coastal waters and lakes.

Optical properties of the natural aquatic environment and underwater solar radiation field are of special interest in investigating radiative, thermal, biological and dynamic processes in water bodies. Solar radiation penetrating water diminishes with depth due to a drastic change in the energy spectrum as a result of absorption by water itself and by its various components. Light provides the energy that drives primary production in the water. Light backscattered from the water column and reflected from its surface gives information for optical remote sensing (about suspended and dissolved substances in the water, turbulent processes, oil pollution etc.). Light absorbed by the water heats the surface layer of the water body. Light absorbed by chemical species provides energy for their dissociation. Light acts as a driving force for fluorescence and photochemical processes. Thus, many vital processes in the water bodies are dependent on light and can be understood with the help of underwater optics.

Problems connected with the estimation of the ecological state of water bodies have become important today due to the increasing human impact on the natural environment as e.g. extensive anthropogenic inputs of nutrients in the water. This can lead to a rapid transition of the water body to a more eutrophic state, which, in turn, entails algal bloom events, anoxia and deterioration of water quality parameters. As known, eutrophication of the water may significantly change the amount and spectral composition of solar radiation penetrating the water body. Thus the optical characteristics of the natural water and underwater radiation field may be considered as indicators of the ecological state of the water body.

Optical remote sensing has become one of the main methods of aquatic environment research, as a tool involving techniques and methods for gathering operative information over large areas and has also been used for monitoring freshwater ecosystems. A signal received by a satellite or airborne sensors originates from the light reflected from the water surface and backscattered from the water column. Therefore, to apply optical remote sensing techniques, an understanding of the underwater light field is needed. It must be noted that interpretation of satellite data is sometimes difficult, not only because of the disturbing influence of the atmosphere and clouds, but also due to some specific features of the objects under investigation (small objects, variation of water properties over short spatial and temporal scales). It must also be noted that optical remote sensing gathers information only from the surface layer of the water body, which can be rather thin in eutrophic water bodies. Consequently, thorough investigation of water bodies is impossible without in situ underwater measurements.

Up to now most of aquatic optical studies have been directed to open ocean waters (Jerlov 1976; Smith and Baker 1981; Sathyendranath et al. 1989; Morel and Gentili 1991; Bricaud et al. 1995; Maffione and Jaffe 1995). However, coastal and inland waters have received increasing attention in recent years (e.g. Kirk 1991, 1994; Kutser, 1997; Maffione

1998; Reinart, 2000; Strömbeck, 2001). The optical variability between inland waters can be much larger than in different regions of open ocean (Horne and Goldman 1994). Inland waters are also optically multicomponent systems. They are characterized by possible high concentration of dissolved organic matter (yellow substance). Part of the yellow substance originates from allochthonous sources, which vary independently from phytoplankton concentration. Also the concentration of suspended inorganic particles can be very high due to river inputs and matter resuspended from the bottom.

There is an essential shortage of field results and valid optical models for multicomponent waters, where different types of dissolved and suspended matter occur often in great concentrations. Due to experimental difficulties in these waters the conclusions obtained from radiative transfer theory are hard to confirm (Kirk, 1994; Mobley, 1994). The optical effect of different components of dissolved organic substances, variable phytoplankton species and nonliving particulate matter is also still under investigation (Bricaud et al., 1995b; Mäekivi and Arst, 1996; Kallio, 1999; Strömbeck, 2001). Much attention is paid to estimation of scattering over all directions in natural waters, especially at small angles in forward and backward directions (Gordon 1991; Ahn et al. 1992; Kirk, 1994). This scattering is a key parameter in analytical models of remote sensing applications. Some of these questions are dealt with in this work.

The environmental remote sensing is generally considered as having begun with the launch of ERTS-1 (Landsat) in 1972. Optical remote sensing of oceanic waters was developed as a science in the seventies and eighties by e.g. Gordon (Gordon, Brown et al., 1975; Gordon, Brown et al., 1988), Sathyendranath (Sathyendranath, 1986) and Bukata, Jerome, Kondratyev and Pozdnyakov (Bukata et al., 1994). A driving force was the development of satellite technology beginning with the Coastal Zone Color Scanner (CZCS) onboard the Nimbus 7 satellite. This was the first optical satellite instrument designed especially for remote sensing of the oceans. The CZCS was replaced by SeaWiFS (onboard SeaStar) and later data from MODIS (Terra) and MERIS (ENVISAT) became available. Remote sensing of lakes has developed in parallel to that of the oceans, but has had a slower start partly due to the satellite sensors having not been very suitable for lake studies (until MERIS) and also due to freshwater science being less organized than oceanography (Dekker, 1993). There is still considerable lack of in-water optical data from freshwaters and in many connections we rely mainly on oceanic data.

Nordic waters were chosen as study sites mainly because: (1) highly reliable data on these lake water properties and quality are urgently needed, (2) lakes and coastal waters are mostly multicomponent systems, being challenging investigation objects, (3) there are thousands of lakes in Finland, Estonia and Sweden, which are important for the economy and recreation. Also the aquatic optical research especially in Finland in a broader perspective is quite young. It was expanded as a co-operation with the Estonian scientists together with the availability of more advanced optical instruments. The co-operation from the Finnish side was initiated by professors Virta and Leppäranta as a Finnish-Estonian project on optical water research, SUVI in 1994. Since 1994 extensive studies and field work has been performed together with the Estonian Marine Institute and the University of Tartu (Arst et al., 1996). The co-operation widened in 1997 as a part of a Research and Development project in EU fourth Framework Program called SALMON (SAtellite Lake MONitoring). The closest partners in SALMON-project were Finnish Environmental Institute, Estonian Marine Institute and the Department of Limnology at the University of Uppsala (Lindell et al., 1999). The work together with all the partners mentioned above is continuing.

The earlier works in aquatic optics in Finland dealt with light penetration in different types of lakes mostly described by the integrated diffuse attenuation coefficient, $K_{d,PAR}$ (Eloranta, 1973; Jones and Arvola, 1984). Later some studies in optics dealt with humic lakes and optical properties of humic substances (yellow substance) (Eloranta, 1999). A slightly more general work dealing with underwater light climate in a lake was commenced by Alberto Blanco in his master's thesis (Blanco, 1994). Of the latest works in aquatic optics can be mentioned a study of absorption properties of yellow substance in Finnish lakes (Kallio, 1999) and remote sensing optical modeling works by Kallio et al. (Kallio et al., 1998; Kallio et al., 2000). In addition studies concerning inherent optical properties and their measurement systems (a flow-through system) connected to water quality monitoring are going on at the division of Geophysics, University of Helsinki (Lindfors and Rasmus, 2000).

This study summarizes author's work in aquatic optics. It is the first extensive work in Finland concentrating on spectral characteristics of optical properties, their mutual relations and hyperspectral modelling in relation to water quality. It provides new information on the optics of boreal waters. It also provides new information about the relationships between inherent and apparent optical properties, spectral characteristics and variations in scattering and backscattering. These are important for optical models and remote sensing of lakes and coastal waters. It is also valuable in providing some new tools and understanding for research and monitoring of water quality in the numerous lakes and coastal sea areas of the Nordic countries. These thoughts and arguments motivated me to include a fairly detailed description of the optical theory in this work.

1.2 Variable coastal waters and lakes

The coastal waters of the Baltic Sea and the boreal lakes are variable in their optical properties. This was seen already in the first extensive optical studies as eighteen lakes in Estonia and nine lakes in Finland were investigated during 1992-97, using mainly optical methods (paper I). The work was initiated by the Estonian Marine Institute and later joined by the University of Helsinki. A total of 200 measurement series were undertaken. The data obtained show a rather high variability in water characteristics, although the investigated lakes are situated in the same climatic region. The chlorophyll *a* and suspended matter concentrations in the surface layer of lakes varied in the limits of 0.3 - 102 mg/m^3 and 1.1 - 145 mg/l, respectively, the effective amount of yellow substance from 1.2 to 150 mg/l. To the depth of 0.5 m penetrates 85 - 5 % of the subsurface solar irradiance in the PAR region, and to the depth of 2 m 56 -0.1 %. Several of these lakes receive human impact, which has more or less influenced the water transparency and the degree of eutrophication. Despite rather low values of attenuation depth in the lakes, water quality can be estimated using optical remote sensing data (e.g. regional water quality maps developed on the basis of Secchi depth by Finnish Environment Institute).

Since the variability of the water properties in inland lakes and coastal waters is very large in the Nordic countries, they are very challenging study objects. Also the density of small lakes is high. Hence there is a lot to be done to increase our knowledge of the optical properties of these kinds of waters, and to understand the relations between the different optical properties of the turbid waters as well as to develop working models for remote sensing and underwater light climate simulations.

1.3 Main objectives of this research

- to study the variability of the different optical properties of natural waters in Finland and Estonia
- to create a long term time series of some basic optical properties (diffuse attenuation coefficient K_d, diffuse reflectance R, absorption a, scattering b and attenuation c of water and Secchi depth Z_S) in five Finnish lakes
- to study the spectral diffuse attenuation coefficient K_d in connection with the underwater light field
- to find relations between different inherent and apparent optical properties
- to study the behavior and spectral characteristics of scattering and backscattering
- to develop and improve hyperspectral models of remote sensing reflectance
- to find practical applications for optical measurements and parameters

1.4 Author's contribution

In papers I-III Helgi Arst was the principal author. In paper I and II Antti Herlevi planned and conducted all spectral measurements of irradiances and data processing. He took part in the field work and research planning, drafted a part of the manuscript and participated in the final compilation. In Paper III Antti Herlevi performed the spectral measurements of irradiances and calculations of diffuse attenuation coefficients and participated as well as planned much of the fieldwork. He took part in research planning and discussions of results (especially concerning the scattering coefficient) as well as in the final compilation of the manuscript. In Paper IV Antti Herlevi was the principal author, responsible for the article and its composition. Helgi Arst was responsible for the calculations of the spectral distribution of scattering. Hanna Virta performed some ac-9 data analysis. Ants Erm participated in the field work and was responsible for the laboratory measurements. Anu Reinart was the principal author of paper V. Antti Herlevi was responsible for all spectral measurements in the field, later data analyses and calculations connected to them. He took part in drafting and compilation of the manuscript. In paper VI Antti Herlevi was responsible and made all the spectral measurements of absorption, attenuation and irradiances and made some calculations connected to them. He took part in planning and compilation of the manuscript. The author is fully responsible for papers VII and VIII, being the only author in those papers.

2 Inherent and Apparent Optical Properties

2.1 Irradiance

The range of electromagnetic wave spectrum to which human eye is sensitive is called light, i.e. wavelengths between 400-750 nm. A similar waveband which drives photosynthesis by phytoplankton is called photosynthetically active radiation (PAR). The incident light, the state of the lake or sea, the bottom conditions and the optical properties of the water itself and its constituents determine the underwater light field.

The basic radiation characteristic is irradiance. It is defined as the radiant flux incident on an infinitesimal element of a surface, containing the point under consideration, divided

by the area of that element. It may also be defined as the radiant flux per unit area of a surface (Eq.1). It has the units Wm^{-2}, or quanta s^{-1} m^{-2}, or mol quanta s^{-1} m^{-2}.

$$E=d\Phi/dS, \tag{1}$$

where Φ is the radiant flux and S is the surface element. Downward irradiance and upward irradiance are the values of the irradiance on the upper and the lower faces, respectively of a horizontal surface.

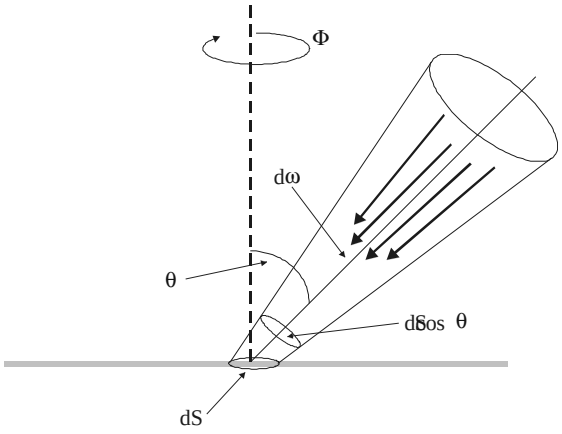

Figure 1. Field radiance at a point in a surface. dS is the area of a surface element, θ is zenith angle, φ is azimuth angle.

The radiance in the direction defined by θ and φ is $L(\theta, \varphi)$ W per unit projected area per steradian (sr) (Fig.1). The projected area of the surface element is d$S\cos\theta$ and the corresponding element of solid angle is dω. The radiant flux on the surface element within the solid angle dω is $L(\theta,\varphi)$d$S\cos\theta$dω. The area of the surface element is dS and so the irradiance at that point in the surface where the element is located, due to radiant flux within dω, is $L(\theta,\varphi)\cos\theta$d$\omega$. The total downward irradiance at that point in the surface is obtained by integrating with respect to solid angle over the whole upper hemisphere

$$E_d = \int_{2\pi} L(\theta,\varphi)\cos\theta d\omega \tag{2}$$

The upward irradiance, E_u, is obtained by integrating with respect to solid angle over the lower hemisphere.

The scalar irradiance E_0 is the integral of the radiance distribution at a point over all directions about the point

$$E_0 = \int_{4\pi} L(\theta,\varphi)d\omega \tag{3}$$

Scalar irradiance is a measure of the radiant intensity at a point, which treats radiation from all directions equally. In the case of irradiance, on the other hand, the contribution of the radiant flux at different angles varies in proportion to the cosine of the zenith angle of incidence of the radiation.

2.2 Apparent optical properties

The apparent optical properties are not properties of the aquatic medium as such, although they are closely dependent on the nature of the aquatic medium. In fact they are properties of the light field, that under the incident solar radiation stream is established within the water body.

We consider first the average cosine, μ, which is a simple quantity that describes the angular distribution of underwater radiance at a given point. It is regarded as the average cosine of the zenith angle of all photons in the particular point, which equals to the ratio of the net irradiance to the scalar irradiance:

$$\mu(z) = \frac{E_d(z) - E_u(z)}{E_0(z)} \tag{4}$$

Its value varies from μ=0 for isotropic (uniform in all directions) radiance distribution to μ=1 for a collimated (narrow angle) beam in downward direction. In natural waters μ is always positive and less than 1

One important apparent optical property, which provides information about the angular structure of the light field, is the irradiance reflectance, *R*. It is the ratio of the upward to the downward irradiance at a given point in the field

$$R(z) = \frac{E_u(z)}{E_d(z)} \tag{5}$$

In any absorbing and scattering medium, natural waters, the irradiances change in value with depth. In a vertically homogeneous water body the values of all spectral irradiances diminish in an approximately exponential manner with depth. Hence we can specify its logarithmic change rate and this will be about the same at all depths. We define the vertical attenuation coefficient for downward irradiance:

$$K_d = -\frac{d \ln E_d}{dz} = -\frac{1}{E_d}\frac{dE_d}{dz} \tag{6}$$

This parameter is most often used for describing optical properties in natural water bodies. The diffuse attenuation coefficients (*K*), the average cosine (μ) and the irradiance reflectance (*R*) are all apparent optical properties, because they depend both on the medium and on the directional structure of the surrounding light field.

2.3 Inherent optical properties

There are two things that can happen to photons within water: they can be absorbed or scattered. The absorption and scattering properties of the aquatic medium for light of any given wavelength are specified by the absorption coefficient, the scattering coefficient and the volume scattering function. They are called inherent optical properties, because their values depend only on the water and its constituents and not on the light field.

They are defined with the help of an imaginary, infinitesimally thin, plane parallel layer of medium, illuminated at right angles by a parallel beam of monochromatic light (Fig. 2). The part of the incident flux, which is absorbed, divided by the thickness of the

layer, is the absorption coefficient, *a*. The part of the flux, which is scattered, divided by the thickness of the layer, is the scattering coefficient, *b*. Beam attenuation coefficient, *c*, is given by

$$c=a+b. \tag{7}$$

The absorption, scattering and beam attenuation coefficients all have units of 1/length, and are normally expressed in m^{-1}.

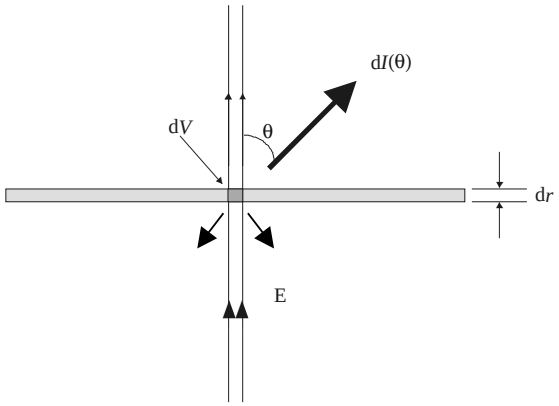

Figure 2. Interaction of a light beam with a thin layer of aquatic medium and also the geometrical relations underlying the volume scattering function. A parallel light beam of irradiance *E* and cross-sectional area d*A* passes through a thin layer of medium, thickness d*r*. d*I*(*θ*) is the radiant intensity due to light scattered at angle *θ*.

The way in which scattering affects the penetration of light into the water depends not only on the scattering coefficient, but also on the angular distribution of the scattered flux. This angular distribution has a characteristic shape for any given medium and is called the volume scattering function *β(θ)*. It is defined as the radiant intensity in a given direction from a volume element (Fig.2). Integrating *β(θ)* over all scattering angles *θ*, gives the spectral scattering coefficient:

$$b = 2\pi \int_0^{\pi} \beta(\theta) \sin\theta d\theta \tag{8}$$

It is useful to divide this into forward, b_f ($0 \le \theta \le \pi/2$) and backward , b_b ($\pi/2 \le \theta \le \pi$) scattering. If we are interested in the shape of the angular distribution of scattering it is convenient to use the normalized volume scattering function, $\tilde{\beta}(\theta)$, sometimes called the scattering phase function, obtained by dividing the volume scattering function by the total scattering coefficient

$$\tilde{\beta}(\theta) = \beta(\theta)/b. \tag{9}$$

3 Radiative Transfer Equation

If we know the properties of the light field and the optical properties of the medium we can ask if it is possible to arrive at relations between them. Although, given an incident light field, the characteristics of the underwater light field are uniquely determined by the properties of the medium, it is still true that explicit all-embracing analytical relations have not yet been derived (Kirk, 1994). This is due to the complex behavior of the photon population in the water caused by the combined effects of absorption and scattering.

It is however, possible to arrive at a useful expression relating the absorption coefficient to the average cosine and the vertical attenuation coefficient for net downward irradiance. In addition, relations have been derived between certain properties of the field and the diffuse optical properties.

Assuming a horizontally stratified water body, with a constant input of monochromatic unpolarized radiation at the surface, and ignoring fluorescence, the change in radiance as a function of depth is:

$$\cos\theta \frac{dL(z,\theta,\varphi)}{dz} = -c(z)L(z,\theta,\varphi) + L^*(z,\theta,\varphi) \tag{10}$$

The term on the left is specified by zenith and azimuthal angles θ and φ. This net change is a resultant of two processes: a loss due to the absorption and scattering and a gain due to the light scattered into a beam (θ,φ) from all directions (θ',φ') (Fig.3). The latter term is called the path function L^* and it is determined by the volume scattering function of the medium. The light field in the water body where there are no internal sources of radiation can be calculated at any depth using Eq. (10), when the angular distribution of incident radiance, the surface conditions, the absorption coefficient and the volume scattering function are known.

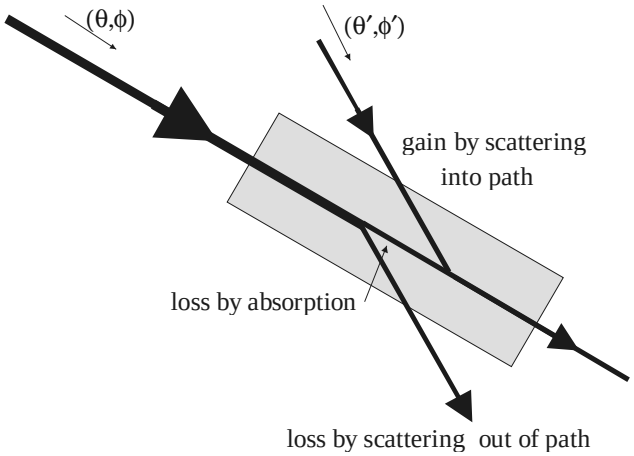

Figure 3. The processes underlying the equation of transfer of radiance.

By integrating each term of Eq. (10) over all angles, we arrive at the relation

$$\frac{d\vec{E}}{dz} = -cE_0 + bE_0 = -aE_0\,, \tag{11}$$

where $\vec{E}$ =E_d-E_u. Eq. (11) is known as the Gershun's law (Mobley 1994). From it follows that

$$a = K_E \frac{\vec{E}}{E_0} \tag{12}$$

and

$$a = K_E \mu \tag{13}$$

This equation relates the absorption coefficient with the attenuation coefficient of net downward irradiance and the average cosine, i.e. a relation between an inherent optical property and two apparent optical properties.

What is the actual nature of the relationship between the apparent and the inherent optical properties? This question is important for two reasons. If we can quantitatively describe in mathematical form the manner in which the inherent optical properties determine the light field, and thus the apparent optical properties, then we have advanced our understanding in the physics of the system. Secondly, the question is of considerable practical importance. Answering the question would enable us to proceed from any anticipated change in the composition of the water to the change in the apparent optical properties, such as the underwater light field available for photosynthesis, or visibility or in the emergent light flux, which is used for remote sensing.

As mentioned, the theoretical equations however are not always applicable to practical purposes, because they need knowledge about the angular distribution of radiation field, which is difficult to measure. Therefore a number of approximate relations between apparent and inherent optical properties based on numerical simulations have been developed by various authors (Gordon et al. 1975; Morel and Prieur 1977; Kirk 1984, 1991; Mobley 1994). For a wide range of inland waters, estuarine and coastal waters the dependence of average K_d over the euphotic zone on the absorption and scattering coefficient is well described by Kirk (1984) (clear sky):

$$K_d = \frac{1}{\mu_0}\left[a^2 + G(\mu_0)ab\right]^{0.5} \tag{14}$$

Where μ_0 is the cosine of the refracted direct solar beam just beneath the water surface. $G(\mu_0)$ is the coefficient determining the relative contribution of scattering to the vertical attenuation of irradiance, and it increases linearly with the increasing of μ_0:

$$G(\mu_0) = g_1\mu_0 - g_2 \tag{15}$$

The parameters g_1 and g_2 depend on the volume scattering function of the water in question. Kirk has also found corresponding relationships for overcast conditions (Kirk 1991).

K_d depends mostly on absorption and varies with the solar zenith angle in proportion to 1/cosθ. Using the above equations Kirk (1984) found that K_d is rather insensitive to the solar zenith angle in highly scattering waters, but in clear oceanic waters with low values of b/a, K_d is likely to vary with the angle of sun up to 41 %.

Gordon et al. (1975) in their Monte Carlo study were able to fit irradiance reflectance just beneath the water surface with the polynomial function of absorption and backscattering coefficients, which can be simplified to

$$R(\lambda) = C(\mu_0)\frac{b_b(\lambda)}{a(\lambda)+b_b(\lambda)} \tag{16}$$

where b_b is backscattering, a is total absorption and C is a coefficient as a function of μ_0, which is a cosine of the zenith angle of the refracted photons. C depends on the solar zenith angle, cloud cover, sea state, and the shape of the volume scattering function. *Kirk* (1984) found in his Monte-Carlo studies the following formula using volume scattering functions of San Diego harbor:

$$C(\mu_0) = 0.975 - 0.629\mu_0 \tag{17}$$

This equation implies that the reflectance decreases as the solar altitude increases. For very clear oceanic waters Gordon (1989) concluded that $R(\lambda)$ is a weak function of θ varying less than 20 % for $0< \theta <60$, but in turbid waters the variation over the same range of zenith angles is as much as 50 % (Reinart, 2000).

4 Influence of the Optically Active Substances to the light field in the water

There are various factors affecting the formation of the underwater light field and that above the water surface. In pure ocean waters there are different salts affecting mainly the ultraviolet part of the spectrum. Real sea or lake water contains a certain amount of phytoplankton and their decomposition products, detritus and dissolved organic matter. Mineral particles originated from land and transported to lake/sea by rivers and wind or resuspended particles from the bottom affect the color of coastal and inland waters. In boreal zone colored dissolved organic matter concentrations are high. It is washed out from soil or originating from the degradation of organic matter in water and has significant influence on the watercolor spectrum. Surface films as well as foam or floating debris of various materials are affecting the remotely measured watercolor, but they may also have an influence on underwater radiation field.

Direct relationships exist between the concentrations of various substances within the water body and the inherent optical properties of the water. In the open sea the influence of terrigeneous material, like sediments and humic substances is negligible from an optical point of view. Phytoplankton are optically a dominant factor even in oligotrophic regions. The coastal and inland waters are multicomponent waters, whose components influence the reflectance spectra in the same wavelengths shadowing each other's influence. How algal cells, dissolved organic material and suspended sediments influence the inherent properties of natural waters is an important question. It is especially so, if one tries to separate the influence of each substance and estimate their concentrations.

4.1 Pure water

The color of pure water comes from the fact that it absorbs only very weakly in the blue and green part of the spectrum, but its absorption begins to rise as wavelength increases above 550 nm and is quite significant in the red region. There is evidence (Pegau and Zaneveld, 1993) that absorption by water is weakly dependent on temperature at least in the red part of the spectrum.

Scattering by pure water is of a density fluctuation type, and so it varies markedly with wavelength. Experimentally, scattering is found to vary in accordance with $\lambda^{-4.32}$ rather than λ^{-4} as predicted by density fluctuation theory alone.

4.2 Colored dissolved organic matter

Colored dissolved organic matter, also called yellow substance, may be land-derived or generated within the water body by decomposition of the phytoplankton. At least close to coastal areas and in lakes the yellow substance is largely land-derived humic material, but in ocean waters away from regions of river discharge the concentration of yellow substance is determined by biological activity averaged over long times. Soluble yellow substances in different natural waters vary not only in molecular size, but also in chemical composition. They all absorb light at the blue end of the spectrum and the spectra are exponential, regardless of their chemical nature.

$$a(\lambda) = a(\lambda_0)e^{-S(\lambda-\lambda_0)}, \tag{18}$$

where $a(\lambda)$ and $a(\lambda_0)$ are absorption coefficients at wavelengths λ and λ_0 nm, and S is a coefficient describing the exponential slope of the absorption curve. For a wide range of seawaters, S has been found to vary between about 0.010 and 0.020 (Bricaud, 1981; Baker and Smith, 1982; Kirk, 1994a; as referenced in Reinart, 2000). The value for Finnish and Estonian lakes and the Baltic Sea has been found to be 0.017 by Mäekivi and Arst (1996) and 0.016 by Kallio (1999).

4.3 Phytoplankton

Phytoplankton are the dominant factor in light attenuation in oceanic waters and often in coastal and inland waters, so it is very important to know the optical properties of algae and other living particles.

Absorption by phytoplankton occurs in various pigments (chlorophylls, carotenoids, biliproteins). They each have a characteristic absorption curve and in different combinations they cover the range of PAR (Kirk, 1994). Typically they absorb light strongly in the blue part of spectrum (430-500 nm) and have a second absorption maximum in the red part (650-680 nm). The absorption curve of phytoplankton population in natural waters is very complex due to variations in pigment composition and "package effect". The distribution of pigments within cells depends on individual species, cell size and the physiological state of phytoplankton (the latter depends also on temperature, nutrients and light availability).

The chlorophyll a occurs in all photosynthetic plants and its concentration is used as a measure of phytoplankton abundance. The values of the specific absorption coefficient of phytoplankton ($a^*_{ph}=a_{ph}/C_{chl}$) presented in literature by various authors, vary greatly. They also exhibit higher values when C_{chl} are small and decrease as C_{chl} increases. Bricaud et al.

(1995b) found an averaged dependence of the specific absorption coefficient of phytoplankton on C_{chl} (0.02-25 μgl^{-1}), taking into account the properties of phytoplankton and the package effect:

$$a^*_{ph}(\lambda) = A(\lambda)C_{chl}{}^{-B(\lambda)} \tag{19}$$

where A and B are tabulated parameters.

Phytoplankton cells and colonies scatter, as well as absorb, light and can make a significant contribution to the total scattering behavior of the aquatic medium. This also varies from one species to another. Algae, such as diatoms and coccolithophores, in which a substantial proportion of the total biomass consists of mineralized cell walls or scales, scatter more than for example naked flagellates. Also blue-green algae with gas vacuoles scatter light much more intensely than those without. The backscattering ratio is generally greater in small cells, such as cyanobacteria than in large eukaryotic cells. Blooms of e.g. coccolithophores have a high backscattering, which seems to contradict the fact that phytoplankton are generally weak backscatterers. This intense upward scattering comes however from numerous detached coccoliths, rather than from the living cells themselves (Morel, 1988; Kirk, 1994b).

4.4 Suspended matter

Suspended matter is not uniquely defined. Often all non-chlorophyllous particles of biological, benthic and/or fluvial origin are summarized as suspended matter or detritus. Kirk (1994) suggests using the term Total Suspended Solids i.e. all the material remaining on a filter pad after filtration of water samples. In this work mostly the concentration of TSS was used.

Nonliving organic particles are produced for example when phytoplankton die and their cells break apart, and when zooplanktons graze on phytoplankton and leave cell fragments and fecal pellets. Their spectral absorption curve has been shown to vary approximately exponentially with a varying slope (Davies-Colley et al., 1988; Bricaud and Stramski, 1990). The relative contribution of detrital absorption tends to decrease if C_{chl} increases.

Inorganic particles consist generally of finely ground quartz sand, clay minerals, or metal oxides in the size range of much less than 1 μm to several tens of micrometers. Their optical influence can sometimes be larger than the influence of organic particles. Such a situation can occur both in turbid coastal waters carrying a heavy sediment load and in very clear oceanic waters that are receiving wind-blown dust. It has been shown that absorption due to inorganic particles has a weak exponential decreasing with increasing wavelength (Dekker 1993).

The particles in natural waters cause an increase in forward scattering at least by four orders of magnitude, and the contribution of density fluctuation scattering to total is notable only in backscattered directions in clear natural waters (Morel and Prieur, 1977). By the results of several studies of volume scattering functions they are similar in shape in clear and moderately turbid waters. In general it is a sharply peaked function and more than 50 % of all scattering takes place at angles less than 5 degrees. The results of Petzold (1972) show that backscattering constitutes 50 % of total scattering in pure water, 4.4 % in the clearest natural water, and about 2 % in turbid water. Scattering depends not only on particle concentration, but also on shape, internal structure, the index of refraction and the size distribution (Kirk, 1994; Jerlov, 1968). The ratio of backscattering to total scattering

for small particles (less than 1 μm, typically mineral) is much higher than for large particles (larger than 1 μm, typically organic). Particle scattering is less sensitive to wavelength than the density fluctuation scattering (Mobley, 1994; Kirk, 1994). In general an increase in scattering is correlated with an increase in total suspended matter, but the coefficient of proportionality and the shape of the spectrum are functions of particle properties (Jerlov, 1968; Kirk, 1994).

5 Passive Optical Remote Sensing

Basically, water color remote sensing is simple. Sunlight, whose spectral properties are known, enters a water body. The spectral character of sunlight is then changed due to absorption and scattering processes in the water, which depend on the type and the concentrations of the constituents in the water body. Part of the changed sunlight eventually makes its way back out of the water and can be detected remotely. If we know how different substances alter sunlight spectra, then we can in principle deduce from these spectra, what substances and how much are present in the water.

The particular light flux, which is of greatest interest, is the upwelling light just below the surface, which succeeds in passing through the surface and certain air layer. As the light passes through the water/air boundary it undergoes refraction, which, in accordance with Snell's law increases its angle to the vertical. A consequence of this is that the flux contained within a small solid angle below the surface spreads out to a larger solid angle above the surface. Because of this effect, the value of emergent radiance at any given angle is about 55 % of the corresponding subsurface radiance. Combining this effect with the much smaller effect of internal reflection, Austin (1980) proposes a factor of 0.544 for relating radiance just above the surface to the corresponding radiance just below the surface. Thus the diffuse component of remote sensing reflectance just above the water surface can be calculated by:

$$r_D(\lambda) = 0.544(0.629\mu_0 + 0.975)\frac{b_b(\lambda)}{a(\lambda) + b_b(\lambda)}. \tag{20}$$

The main significance of the values of upward radiance lies in what they can tell us about the optical properties of the medium, and thus about the concentrations of the optically active substances.

The inherent optical properties (IOP's) are dependent on the different optically active substances (OAS) in the water and follow Beer's law. This means that they are proportional to the concentrations of the OAS. We assume that there are three optically active substances in the water: phytoplankton pigments, yellow substance and suspended matter. Under these conditions the total spectral absorption coefficient of the water, $a(\lambda)$ is described by the following formula:

$$a(\lambda) = a_w(\lambda) + a^*_{ph}(\lambda)C_{chl} + a^*_y(\lambda)C_y + a^*_{SM}(\lambda)C_{SM} \tag{21}$$

where a^*_{ph} is the chlorophyll-specific spectral absorption coefficient of phytoplankton, a^*_y and a^*_{SM} are spectral specific absorption coefficients for yellow substance and non-chlorophyllous particles, respectively; and C_{chl}, C_y and C_{SM} are concentrations of chlorophyll a, yellow substance and non-chlorophyllous suspended matter.

The total spectral backscattering coefficient $b_b(\lambda)$ can be described by the formula:

$$b_b(\lambda) = 0.5b_w(\lambda) + b^*_{b,ph}(\lambda)C_{chl} + b^*_{b,SM}(\lambda)C_{SM} \quad (22)$$

where b_w is the scattering coefficient of pure water and it is assumed that backscattering probability is 50 % in pure water. $b^*_{b,ph}$ is chlorophyll-specific backscattering spectrum and $b^*_{b,SM}$ is spectral backscattering coefficient of non-chlorophyllous suspended matter.

In the semi-analytical approach (in-water optical model) equations (18-22) are used to interpret the remote sensing data. In this the OAS concentrations are as input and the equations give estimates of radiance reflectance as the output. They can also be used in the reverse way, i.e. to determine the concentrations of the optically active water quality parameters from a spectrum of irradiance reflectance. This is called inverse modeling. These models have been proven to be suitable for interpreting remote sensing data if the relations between the water quality parameters and inherent optical properties are known well enough. It means that the selection of proper specific absorption and scattering coefficients spectra for calculating $a(\lambda)$ and $b_b(\lambda)$ is crucial and difficult.

The second approach in remote sensing is an empirical method, where remote sensing data is related to measurements of water quality parameters by regression analysis. The relations have been developed between radiances in particular wavebands or functions of one or more radiances and the concentrations of OAS. This approach requires extensive fieldwork and logistics since samples have to be collected from the water almost simultaneously with the measurements of the remote sensor. The advantage of this method is that even though few parameters are measured, it can be very accurate locally during one particular campaign. The derived algorithms are not expected to be generally valid.

6 Measurements and Equipment

6.1 Sites

The lakes under regular study during this work are situated in the southern Finland and Northern and Southeastern Estonia. There were however some episodic studies in numerous small lakes in Estonia and a few in southern Finland. Some additional test sites in lakes in Finnish Lapland near city of Rovaniemi and two sites in the Gulf of Finland, Baltic Sea were studied too. Also measurements in Sweden were performed in lake Erken and in the Baltic Sea area outside Norrtälje in 1998 and 1999 and in lake Vänern in 2001. All in all there was data gathered from 34 lakes and additionally from 4 sites in the Baltic Sea. Extensive measurements in 12 Finnish lakes were carried out during the European Union project SALMON (summers 1997-1998) and less complex, but regular measurements during a Finnish-Estonian project SUVI (summers 1994-2000). Lakes were selected on the basis of previous knowledge of their optical properties and trophic status. They represent typical different types and sizes of waterbodies in the boreal ecoregion varying from very turbid hypertrophic lakes to clear oligotrophic lakes. The bio-optical characteristics show considerable variation making these waters challenging study objects at least in the respect of finding good model parameters for bio-optical models and correlations between different optical properties. The most important bio-optical characteristics are the concentrations of chlorophyll C_{chl} and suspended matter C_s, an effective concentration of yellow substance C_y (calculated from absorption of yellow substance) and Secchi depth Z_s. Additional information about these lakes can be found in paper I. In this text most of the relevant parameters are calculated from data of the 12 lakes studied regularly (Table 1). The positions of these lakes are shown in Fig.4.

Table 1. Mean values of Secchi depth (Z_S, m), concentrations of suspended matter (C_S, mgl^{-1}), chlorophyll a (C_{Chl}, mgm^{-3}) and yellow substance (C_y, mgl^{-1}), integrated beam attenuation coefficient in PAR (c, m^{-1}) in Finnish and Estonian lakes in 1995–2000. The numbers refer to lake numbers shown in Fig. 4.

LAKE	C_S,*mg/l*	C_{chl},mgm^{-3}	C_y, *mg/l*	*c(mean)*,m^{-1}	Z_S, *m*
1 Päijänne	1.14	3.53	7.43	1.22	5.21
2 Pääjärvi	2.97	9.91	20.33	3.03	2.55
3 Vesijärvi 1	2.41	8.54	4.82	1.91	2.74
3 Vesijärvi 5	3.53	12.68	4.89	2.11	2.55
4 Keravanjärvi	1.71	13.8	33.3	5.34	1.2
5 Tuusulanjärvi	19.69	35.54	17.34	12.21	0.64
6 Lohjanjärvi 2	9.66	30.68	18.97	6.37	0.95
6 Lohjanjärvi 5	5.54	18.35	14.88	4.42	1.36
6 Lohjanjärvi 6	4.09	10.85	11.16	3.20	1.10
7 Ülemiste	19.7	61.3	11.4	12.4	0.7
8 Paukjärv	2.10	7.50	1.81	0.97	4.90
9 Võrtsjärv	13.86	45.48	14.71	12.05	0.75
10 Verevijärv	5.88	26.20	11.00	3.66	2.21
11 K. Valgjärv	1.99	11.43	4.58	1.90	4.21
12 N. Valgjärv	2.77	9.00	5.09	1.77	4.38

Figure 4. The positions of 12 the lakes in Estonia and Finland that were studied regularly during this work. The visible light image is taken by a MODIS instrument onboard Terra satellite (©NASA).

6.2 Measurements

The determined limnological parameters, used in this work, were: concentration of total suspended matter (C_S), the sum of chlorophyll-*a* and phaeophytin-*a* (further chlorophyll-a, C_{Chl}) and the absorption coefficient of filtered water samples (a measure of yellow substance or colored dissolved organic matter, a_Y), using Sartorius cellulose acetate filters, with 0.45 μm pore diameter. Concentrations of chlorophyll were measured using Whatman GF/C filters and pigments were extracted with hot ethanol. Full absorption spectra (350-850 nm) of the yellow substance were measured in a laboratory using Hitachi U-1000 (SUVI project) and Shimadzu UV-PC2101 and Perkin-Elmer Lambda spectrophotometers (SALMON project). The concentrations of suspended matter were measured in water samples using gravimetric determination with 0.45 μm Sartorius cellulose acetate filters (SUVI project) and 0.4 μm Nuclepore filter (SALMON project).

The integral downwelling irradiance was measured using three underwater sensors, which measure the integral radiation in the PAR waveband: two LI-192SA: s (for vector irradiance) and LI-193 SA (for scalar irradiance). The LI-192 SA sensors were mounted on a frame with a 0.5 m vertical distance between them to determine the attenuation coefficient.

Vertical profiles of the spectral absorption and attenuation coefficients were measured with a WetLabs ac-9 absorption/attenuation meter. We used the standard wavelength channels of ac-9: 412, 440, 488, 510, 532, 555, 650, 676 and 715 nm in 1997-1999 and 2000-2001 the channel 532 nm was omitted and 630 nm was included. A Li-Cor Li-1800UW spectrometer was used to measure downwelling and upwelling spectral irradiance profiles in the water with 2 nm spectral resolution in the wavelength band of 300-850 nm.

6.2.1 Instruments and accuracy

LI-1800UW spectroradiometer

A portable scanning spectroradiometer Li-1800UW manufactured by LI-COR Corporation was used to provide the spectral vector irradiance. The data in $Wm^{-2}nm^{-1}$, can be converted to quanta $s^{-1}m^{-2}$, the quantity used in photosynthetic studies. Underwater scan limits for this instrument are from 300 to 850 nm, while in the air the range is from 300 to 1100 nm. During the study the scans were taken at 2 nm intervals. Radiation enters the detector through a cosine receptor, which enables a 180-degree uptake. For the monitoring of the upwelling spectral irradiance, the instrument must be turned around and lowered detector facing downward.

The spectral irradiance above the water surface must be known in order to obtain consistent data of underwater spectral irradiance at different times. However, the intensity of the global radiation can be used as the indicator for the spectral irradiance, because the spectral distribution of the incoming irradiance does not vary significantly within the time span of noon ± 3 hours. As the global radiation may vary considerably due to the variation in the cloud cover, this radiation ought to be measured at the same time and preferably at the same place as the underwater irradiance. In this study a Li-200SA photodiode sensor with a Li-1000 data logger was used to measure the total incident irradiance (i.e. global sun plus sky radiation) in the range of 400-1100 nm.

The effect of waves on the underwater spectral measurements is another serious source of error. In our case the only method for correcting their effects is smoothing the

spectrum. The more modern instruments can measure an irradiance spectrum very quickly and the effect of wind can be eliminated by measuring the spectrum several times and then computing averages over these spectra.

The measurement accuracy of the Li-1800UW is 3 to 10 % (depending on wavelength) relative to a standard supplied by the U.S. National Institute of Standards and Technology (NIST). Instrument drift with time will add to the uncertainties. In order to maintain the instrument within its specified accuracy, recalibration is recommended every 6 months. This can be accomplished using the 1800-02 Optical Radiation Calibrator.

ac-9 absorption/attenuation meter (see also paper IV)

The ac-9 is a spectral absorption/attenuation meter that uses nine band-pass filters to spectrally discriminate the light from a tungsten lamp (hence the name of the instrument from *a*, absorption, *c*, attenuation in 9 channels). The wavelengths most often used are 412, 440, 488, 510, 532, 555, 650, 676 and 715. The basic system components necessary to operate the ac-9 are shown in Figure 1. in paper IV.

The ac-9 unit consists of two pressure housings separated by three stand-offs. The shorter of the two pressure cylinders houses the light sources, filter wheel and transmitter optics. The longer of the two cans houses the receiver optics and the control and acquisition electronics for the unit. The absorption and attenuation beam paths and flow tube assemblies are between the receiver and transmitter housings.

The ac-9 performs simultaneous measurements of the water's attenuation and absorption characteristics by incorporating a dual path optical configuration in one instrument. Each path contains its own source, optics and detectors and the two paths share common filter wheel and control and acquisition electronics. The beam performing the attenuation measurement is referred to as the **c beam** and the beam used to make the absorption measurement as the **a beam**. The accuracy of the ac-9 instrument is $\pm$ 0.005 m^{-1}, if checked and calibrated regularly.

<u>c beam</u>

The beam passes through a pressure window into the sample water volume. A flow tube encloses the water path. Scattered light which hits the blackened surface of the flow tube is absorbed and therefore does not contribute to the measurement of transmitted intensity. Light radiated through the flow path is therefore subject to both scattering and absorptive losses by the water.

<u>a-beam</u>

The sample water volume is enclosed by a reflective flow tube. Light passing through the tube is both absorbed by the water itself and by various pigments within the sample. Forward scattered light is reflected back into the water volume by the reflective tube. The light is then collected by a diffused large area detector at the far end of the flow tube.

HS-6

The backscattering measurements were performed by a HOBI Labs Hydroscat-6 b_b-meter (HS-6). It has six channels, which are centered around 442, 470, 510, 589, 620 and 671 nm. The optical unit consists of 12 quartz or acrylic glass windows on the faceplate of the instrument. For each channel, cone shaped light beam of about 8 degrees divergence is

sent out through one of the windows into the water in an angle of about 71 degrees from the faceplate towards the center axis of the instrument. The backscattered light is detected through a second window by a receiver with an acceptance angle of 8 degrees and an angle of 71 degrees towards the centerline. Thus the instrument measures backscattering at an angle of about 142 degrees. As the light passes through the water and is backscattered back into the instrument, it is attenuated. Therefore the raw measurements need to be corrected. The correction method is described in Strömbeck (2001). The HS-6 was used simultaneously with the ac-9 to determine the backscattering probabilities as vertical profiles or continuous flow-through measurements.

The total irradiance sensors are simple with a reasonable accuracy due to a silicon photodiode, but the response of the silicon photodiode is not ideal. The response does not extend uniformly over the full solar radiation range. The Li-200SA sensor has been calibrated against an Eppley Precision Spectral Pyranometer (PSP). The absolute error under natural daylight conditions is 5 % maximum, typically 3 %. The same applies for the other photodiode sensors Li-192SA and Li-193SA that were used to measure underwater irradiances.

The spectrometer Hitachi U1000 is designed for measuring the difference between the absorption coefficient of some solution and that of distilled water. In reality a small-angle forward scattering does reach the detector and contribute in the measured value of the beam attenuation coefficient (Eq. 1 in I). Given the detector acceptance angle (0.9º) in the Sea-Tech transmissometers, it was found that the difference between the measured and real $c(\lambda)$ is 4-10 % of the total b for various volume scattering functions (Zaneveld et al. 1992). By our estimations the acceptance angle for Hitachi exceeds that for Sea-Tech, so for Hitachi the difference between the measured and real $c(\lambda)$ is most likely more (24 % when compared to the average attenuation values measured with ac-9).

6.2.2 Measurement methods

All the measurements were performed from a boat. For Li-1800 UW measurements a 3 m long support was used to hold the instrument away from the boat (figure 5). The instrument was lowered with a rope and controlled with a terminal connected to the instrument. To avoid any shadows, the boat was turned so that the sun was on the instrument's side.

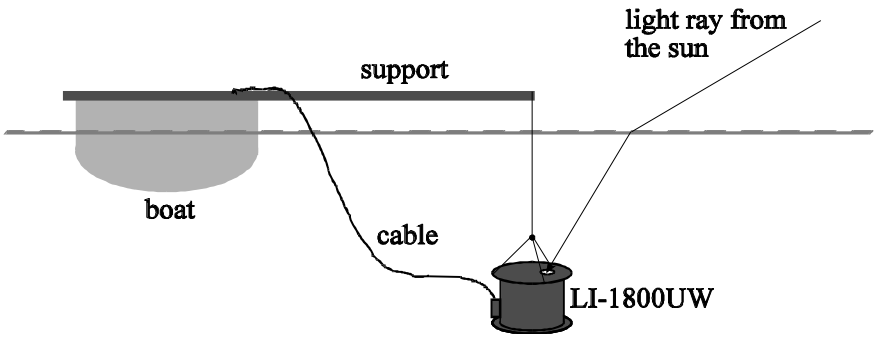

Figure 5. The measurement configuration of the Li-1800 UW spectroradiometer.

The downwelling spectral irradiance was determined generally at depths 0.5, 1, 1.5, 2, 2.5, 3 and 4 m and 5 and 6 m in the clearest lakes. The upwelling irradiance was measured similarly in 0.5, 1, 1.5, 2, 2.5 and 3 m. In order to improve the reliability of the

measurements and understanding the disturbing effects caused by clouds and waves to the underwater light field, two scans were taken at each depth. During all underwater measurements the Li-200SA sensor attached to a Li-1000 data logger was mounted on the boat. It measured the total incident irradiance in one-minute averages. As each scan takes about 40 seconds to be completed and we measured more or less every minute, the data collection at one point including the measurements in the air took about 45 minutes.

The ac-9 measures rapidly allowing near continuous depth profiles to be measured. Generally three in situ profiles of attenuation and absorption were measured at every sample point.

Measurements for the profiles of integral downwelling irradiance (PAR) in the water and water samples were taken simultaneously with the Li-1800UW measurements to get the best possible data for comparison and calibration.

6.3 Data processing

6.3.1 Li-1800UW

Li-1800UW data was evaluated specially bearing in mind the changing weather conditions. The variation in the incident downwelling radiation both during one measurement (one scan) and the whole measurement series at one point was dealt with in the following manner.

As explained in the previous chapter the Li-200SA sensor measured the total incident irradiance in one-minute averages. The Li-1800UW measurement time for a given depth was 40 seconds. If the consecutive values of the total irradiance recordings were changing by more than 20 % of the average over the whole measurement series the corresponding Li-1800UW measurement was left out of the data-analysis. Further to eliminate the effect of the variations in the incident downwelling radiation that occured during the whole measurement series (duration about 45 minutes) a correction coefficient for each underwater spectrum was calculated according to Eq. 23 (Virta and Herlevi, 1999).

$$c = \frac{E_d^{ave}(Li-200)}{E_d^{i}(Li-200)} \tag{23}$$

where E_d is the incident irradiance measured by Li-200SA (an average during the whole measurement series respective 1 minute values). The normalized spectra are obtained by multiplying each measured spectra by the correction coefficient c.

Not only clouds, but even small waves can cause strong fluctuations in the underwater irradiance, due to varying angles with which the incoming light rays penetrate the water surface. Because of this two methods were used to smooth out the effects of the waves: filtering with a low pass filter and a polynomial fitting to the measured spectrum. Because the error seems to be proportional to the level of irradiance, the smoothing was applied to logarithmically transformed spectra.

The irradiance spectrum in a wavelength domain can be considered as a spectrum in the time domain, the wavelength interval 2 nm corresponding to the time interval of 2x40/550 s = 145 ms. Because the period of wind waves is about 1-2 s, the effect of waves can be filtered by a low pass filter with the limit period of the order of 2 s. We used a Butterworth recursive filter (Krauss et al., 1994), with a length of 3. It includes 5 parameters and filtering was made twice, first advancing with the increasing time and then in the opposite direction. The parameters of the filter depend on the selected cut off frequency.

Another possibility of smoothing the measured spectrum is to apply polynomial fitting to the data. It was observed that a polynomial having degree14 or 15 should be used. The testing of the smoothing procedure suggest that when the disturbance is low the low pass filtered series seems to give better consistency with the measured series than the polynomial fit. In case of higher disturbance the situation may be the opposite. However, the difference between these two smoothing methods is not large.

6.3.2 ac-9

ac-9 data was post-processed, i.e. corrected for temperature and scattering effects. The absorption coefficient measured by the ac-9 is the difference between the absorption coefficient of the optically pure water used as a reference in calibrating the ac-9 and the absorption coefficient of the water in which the measurements are being made. By referencing the ac-9 measurement to pure water, the measured absorption (a_m) and attenuation (c_m) coefficients represent the total absorption (a_t) or attenuation (c_t) minus the absorption (a_{wr}) or attenuation (c_{wr}) coefficient of water.

$$a_m = a_t - a_{wr}, \qquad c_m = c_t - c_{wr} \tag{24}$$

It has been shown that the absorption coefficient of water is dependent on temperature and salinity in some portions of the spectrum. The temperature and salinity effects are largest in the near infrared and at the shoulders of the absorption spectrum in the visible. Temperature (t) and salinity (S) effects can be removed using a simple algorithm:

$$a_{mt} = a_m - \left[\Psi_t^*(t - t_r) + \Psi_S^*(S - S_r)\right] \tag{25}$$

where the values for Ψ_t and Ψ_S are given in tables. The effect of salinity is small compared to temperature and in our lake and brackish waters it has been omitted.

Attenuation measurements are limited by the acceptance angle of the instrument. The finite acceptance angle of the instrument means that it collects a portion of the scattered light and thus underestimates the true attenuation coefficient. However correcting attenuation measurements due to scattering is not recommended as it is extremely difficult and of questionable benefit.

Reflecting tube absorption meters and spectrophotometers do not collect all of the light scattered from the beam. The uncollected scattered light causes the instrumentation to overestimate the absorption coefficient. There are several schemes to correct absorption measurements for scattering errors. The three methods most commonly used include:

-subtraction at all wavelengths of a constant absorption based on that measured at the reference wavelength where the absorption is assumed to be zero.

-removal of a fixed proportion of the scattering coefficient.

-use of a reference wavelength to determine the proportion of the scattering coefficient to be subtracted from the signal.

Each of these methods requires different assumptions and ancillary measurements. We have used the third type of correction in which it is assumed that there exists a reference wavelength (λ_{ref} = 715 nm in this study) at which the absorption coefficient of particulate and dissolved materials is zero. It is further assumed that the shape of the volume scattering function is independent of wavelength. The correction technique is written as,

$$a_t(\lambda) - a_w(\lambda) = a_m(\lambda) - \frac{a_{mt}(\lambda_{ref})}{c_{mt}(\lambda_{ref}) - a_{mt}(\lambda_{ref})} * [c_m(\lambda) - a_m(\lambda)] \quad (26)$$

This technique allows for automatic changes in the scattering correction magnitude with wavelength and changes in types of materials present and it is the most accurate of the techniques.

Since the ac-9 measurements are referenced to optically pure water, it is necessary to add the optical properties of the reference water to arrive at the total absorption or attenuation coefficient. The absorption and attenuation coefficients of pure water recommended by WET-Labs can be found in ac-9 Protocol (2000).

7 Results and Discussion

7.1 Variability in the optical properties

As mentioned already in the introduction, the variability in the water properties may be remarkable in lakes and coastal areas in the Boreal ecoregion. This chapter describes the general variability in different optical parameters, their temporal and spatial variations and finally some classifications based on underwater reflectance spectra. Looking at the whole data set collected during the years between 1994 and 2001 it can be concluded that the variation in the optical properties is large both through time and space. Table 2 in paper I shows the minimum and maximum values of Secchi depths, and the concentrations of chlorophyll, yellow substance, and suspended matter in 1992-1997. Considering the Secchi disk values it can be seen that the lakes under consideration were of low transparency (< 7m), compared to the oceans, except for two lakes, Lake Äntu Sinijärv (15 m) and Vasikkajärvi (10) (measured in 1998 and not shown in Table 2). In some lakes the variation was much more than in others, e.g. C_{Chl} for Lake Lohjanjärvi changed from 8.5 to 64.5 mg m^{-3}, but for Lake Päijänne only from 1.3 to 1.7 mg m^{-3}. Two strongly turbid lakes - Võrtsjärv and Tuusulanjärvi- showed different variability limits for suspended matter: for Võrtsjärv it was from 5 to 145 mg l^{-1}, for Tuusulanjärvi from 12 to 37.5 mg l^{-1}.

Lake Lohjanjärvi showed comparatively high variability in all parameters, whereas e.g. Lake Päijänne seemed rather stable, showing that some lakes have more stable bio-optical properties than others. The variation in the sea areas and the sites in Sweden could not be followed due to too few measurements.

The same conclusion about the variations can be drawn considering the values of e.g. the attenuation coefficient measured by the Hitachi spectrophotometer, c^*(400-700) or the Secchi depth, Z_S for each lake. The c^* is a sensitive measure of water transparency. Such sensitivity was estimated by means of the relative variation δ(x):

$$\delta(x) = \frac{2(x_{\max} - x_{\min})}{x_{\max} + x_{\min}}, \quad (27)$$

where x stands for the value of Z_S or c^*(400-700). The following results were obtained: $\delta(Z_S)$<60% for 13 lakes and 60-130% for 9 lakes, but $\delta[c^*(400\text{-}700)]$<60% only for 7 lakes and 60-160% for 15 lakes.

A widely used optical property, that was intensively studied in this work, is the diffuse attenuation coefficient (K_d) (Eq.6). Different combinations of substances are responsible

for light attenuation in different lakes. The average values of integrated attenuation coefficient in the PAR region, $K_{d,PAR}$ varied from 0.2 m^{-1} in Lake Äntu Sinijärv to 7.2 m^{-1} in Lake Nohipalu Mustjärv. Sometimes $K_{d,PAR}$ was also observed to be highly variable during the warm season even in one lake. We computed also the light transmittance function using the following equation:

$$\tau(z) = \frac{E_d(z)}{E_d(z=-0)} \tag{28}$$

The results show what proportion of the subsurface PAR-radiation reached different depths. The numerical values for 14 lakes are shown in Fig.6.

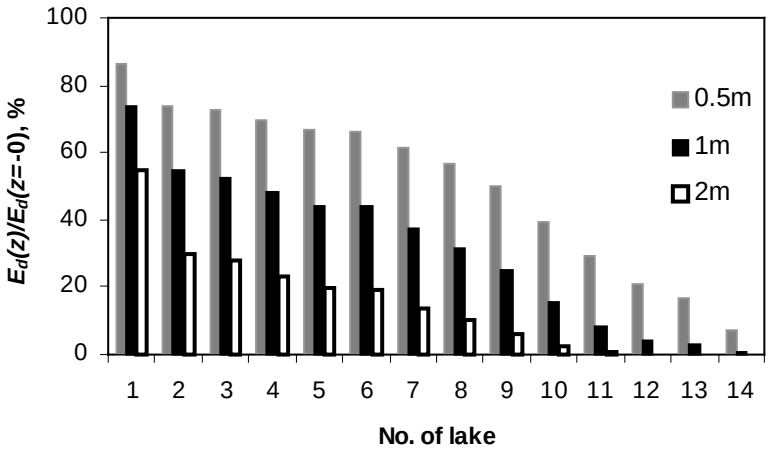

Figure 6. The values of Ed(z)/Ed(z=-0) (in per cents), computed from Kd(PAR), averaged for each lake: 1. Lake Äntu Sinijärv; 2. Lake Koorküla Valgjärv; 3. Lake Nohipalu Valgjärv 4. Lake Päijänne; 5. Lake Kurtna Nõmmejärv; 6. Lake Vesijärvi;7. Lake Verevi; 8. Lake Lohjanjärvi; 9. Lake Pääjärvi; 10. Lake Uljaste; 11. Lake Võrtsjärv; 12. Lake Valkeakotinen; 13. Lake Tuusulanjärvi; 14. Lake Nohipalu Mustjärv.

Studying the inherent optical properties, absorption, scattering and attenuation, measured with ac-9, one can again see the large variation between the lakes, Figs. 2-4 in paper IV. The beam attenuation at λ=412 nm varied between 2 and 28 ($c1$ and $c11$ in Fig. 2 a, b) and the shapes of the spectra varied considerably depending on the dominating optically active substances (suspended matter, chlorophyll-a or yellow substance).

The variation during the summer was quite large in some lakes and it could also be seen from the results of the IOP:s (papers IV and VIII). In general the results showed that there was more yellow substance and smaller particles present and higher turbidity in May, while in August larger particles and lower scattering levels were found. In the spring after the snowmelt the water contains relatively more small mineral particles while in August the amount in algae is larger. Also the waters were more unstratified in May, whereas in August layering, peaks and effects of thermoclines could be seen in the water column (IV).

The yearly variation of integrated diffuse and beam attenuation coefficients, K_d and c, was studied both in Finland and Estonia. The results from the Finnish lakes are shown here in Figs.7-8. They show large, but somewhat arbitrary variations in these parameters from year to year. E.g. Lake Tuusulanjärvi was most turbid in 1997 and getting somewhat clearer after that, in lake Lohjanjärvi the water quality seemed to improve slightly and lakes Päijänne and Pääjärvi were quite stable. There was some indication that the water in

lake Vesijärvi got somewhat more turbid during the years. The variations in Estonia were also quite large, but no clear tendencies could be detected. These time series are however too short and too infrequent to make any final conclusions about any possible trends in the annual changes in these waters. The regular measurements of underwater irradiances and absorption and beam attenuation are continuing in the following 5 Finnish lakes: Päijänne, Vesijärvi, Pääjärvi, Tuusulanjärvi and Lohjanjärvi.

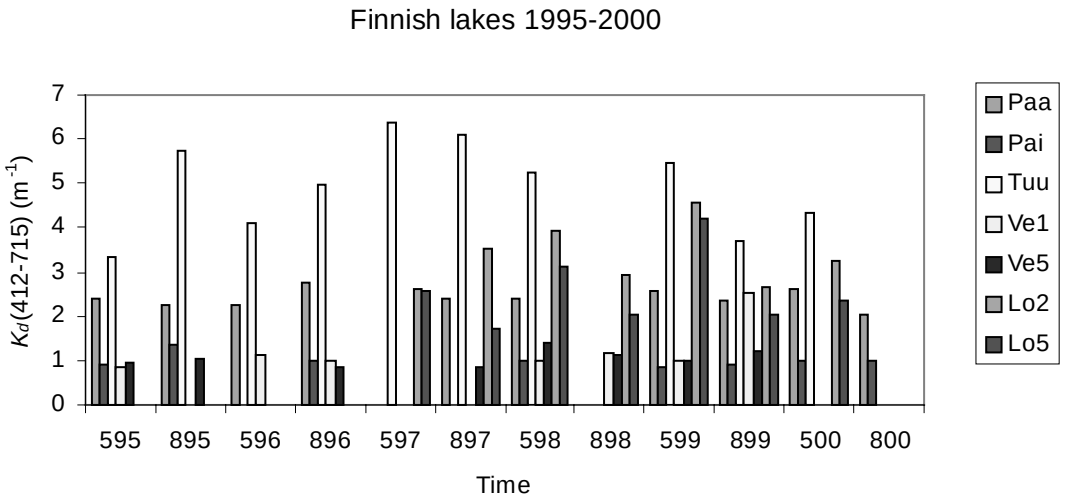

Figure 7. The yearly variation of integrated diffuse attenuation coefficient, K_d in 5 Finnish lakes during 1995-2000. In the legend Paa=Lake Pääjärvi, Pai=Lake Päijänne, Tuu=Lake Tuusulanjärvi, Ve1(5)=Lake Vesijärvi, point 1(5), Lo2(5)=Lake Lohjanjärvi, point 2(5).

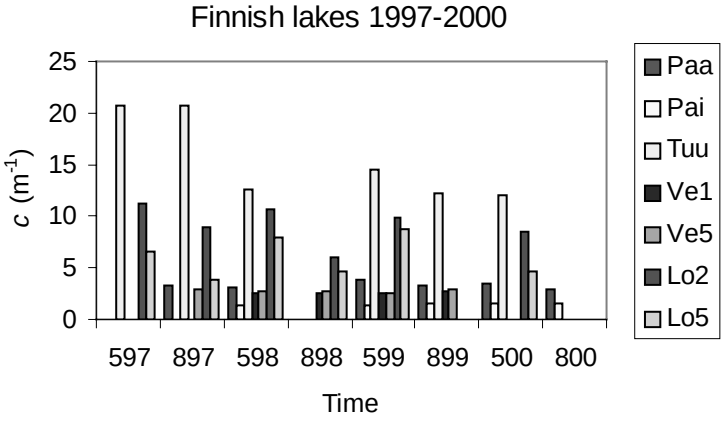

Figure 8. The yearly variation of integrated beam attenuation coefficient, c in 5 Finnish lakes during 1997-2000. In the legend Paa=Lake Pääjärvi, Pai=Lake Päijänne, Tuu=Lake Tuusulanjärvi, Ve1(5)=Lake Vesijärvi, point 1(5), Lo2(5)=Lake Lohjanjärvi, point 2(5).

Spectral K_d gives more information about the underwater light field than the broadband K_d. One example for each lake was chosen to show the variability in our lakes, Fig.9 here and Fig.4 in paper V. The figures show the different values and shapes of the spectra representing different water types. The differences are clear going from clear to turbid and brown waters (as explained on pages 275-276 in paper V).

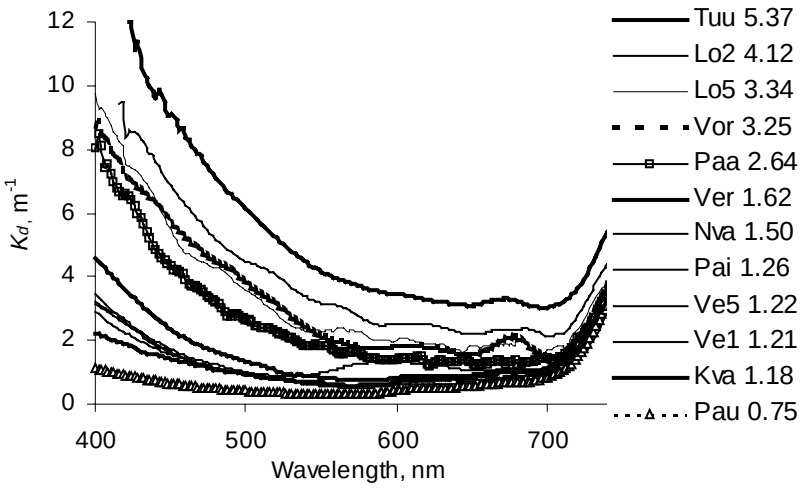

Figure 9. Representative examples of the spectral attenuation coefficient, K_d in Finnish and Estonian lakes. In the legend Tuu=Lake Tuusulanjärvi, Lo2(5)=Lake Lohjanjärvi, point 2(5), Vor=Lake Vortsjärv, Paa=Lake Pääjärvi, Ver=Lake Verevi, Nva=Lake Nohipalu Valgjärv, Pai=Lake Päijänne, Ve1(5)=Lake Vesijärvi, point 1(5), Kva=Lake Koorkula Valgjärv, Pau=Lake Paukjärv. The numbers in the legend refer to integrated values of K_d.

Any increase in the concentration of optically active substances (including temporal changes due to phytoplankton bloom, yellow substance transport at spring, suspended particles from the shore after heavy rains) increase the diffuse attenuation coefficient and change its spectral composition. In clear lakes, Sinijärv, Vasikkajärvi, Päijänne, Puujärvi, Paukjärv, Valgjärv, the wavelength of maximum penetration λ_{max} varies from 520 nm to 578 nm and the respective penetration depth ($z_k = 1/K_d$) from 9.2 m to 2.4 m. In moderately turbid lakes Vesijärvi, Verevi and Pääjärvi the maximum penetration depth is 1.1 – 2.9 m in the spectral region of 580-670 nm. In shallow and turbid lakes Võrtsjärv and Tuusulanjärvi, rich in phytoplankton, the most penetrating wavelengths are 590-650 nm and z_k=0.5-0.8 m. In very brown-water lakes N. Mustjärv and Valkeakotinen λ_{max} is shifted to the red part of the spectrum (about 710 nm) and the layer available by remote sensing methods is very thin: 0.3-0.6 m.

Spectral variations of the irradiance reflectance, *R*, were also studied. One representative curve for each of the regularly studied lakes is presented in Fig. 10. One classification of lakes by the irradiance reflectance is proposed by Vertucci and Likens (1989), relying on the measurements carried out on Andirondack Mountain lakes. They divided these lakes into five types according to the shape of the reflectance spectra. In our lakes the amount of optically active substances is often much higher than in the lakes studied by Vertucci and Likens. Several types of reflection based classifications can be made, one is introduced by Reinart (2000), based on Vertucci and Likens. The study was based on data from Estonian and Finnish lakes (47 reflectance spectra). The data was divided into five types, 3 (clear)-7 (brown) according to their reflectance spectra (types 1 and 2 could not be found in our waters). A detailed description of the different water types can be found in pages 48-50 and Fig. 6 in Reinart (2000). Another simple classification was performed in this study where the lakes were divided into **V**ery turbid (5), **T**urbid (5), **M**oderate (4), **C**lear (3) and **B**rown (6) types (see Fig.6). The numbers in parenthesis refer to the types introduced by Reinart (2000).

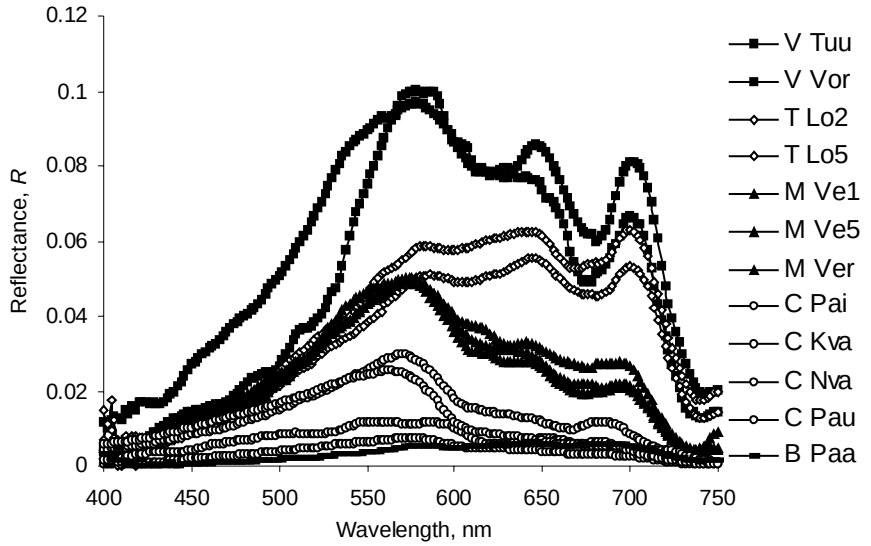

Figure 10. Representative examples of the spectral irradiance reflectance, *R* in Finnish and Estonian lakes. The letters in the legend refer to water types **V**ery turbid, **T**urbid, **M**oderate, **C**lear and **B**rown. For the lake names see figure text in Fig. 9.

7.2 Inherent and Apparent Optical Properties (IOP, AOP)

The apparent optical properties of a water body are the product of the interaction between the incident solar flux and the inherent optical properties of the water. Documenting the various inherent and apparent optical properties and their relationships to each other in Finnish and Estonian lakes was one of the main goals of this work. They were measured since 1994 in various types of waters, both in lakes and coastal waters, as seen in the previous chapter. The relationships as mentioned in chapter 3 between AOP: s and IOP: s are important for two reasons: if solved they help us understand the overall light field under water much better and the physics that govern the relations, secondly they have a very important practical purpose. They enable us to proceed from any anticipated change in the composition of the water to the change in the apparent optical properties, such as the underwater light field available for photosynthesis, or visibility or in the emergent light flux, which is used for remote sensing. The reason for this is that the value of an inherent optical property, due to a particular component of the medium, is linearly related to the concentration of that component.

The diffuse attenuation coefficient was an optical property that was studied most intensively during this work. The values of K_d are useful because: (1) they are easily determined with standard instruments; (2) they generally correlate well with optically active substances in the water; (3) they are related to inherent optical properties of the water; (4) the lower limit of the euphotic zone within which significant photosynthesis occurs can be calculated as $4.6/K_d$; (5) they give importance for remote sensing, as 90 % of the remotely sensed radiation originates from the layer with a thickness of K_d^{-1} (e.g. Kirk, 1994).

7.2.1 Integral values of Z_S and K_d and c

The correlative relationships between the total beam attenuation coefficients in the PAR region and Secchi depth are shown in Fig. 2 in paper I and in Fig. 11 here. The latter result was found to be $c=8.4/Z_S$ (n=66, R=0.94, $p<5.7\cdot10^{-33}$). The first has been measured by a

spectrophotometer from water samples during 1992-1997 and the second by an ac-9 in 1997-2000. In both cases the correlation was good R>0.88, but the equation in Fig. 2 gives smaller values for *c* than the relation mentioned above. This indicates again that the spectrophotometer gives too small values for *c*. However, the conclusion can be drawn that the mean beam attenuation coefficient can be suitable as an indicator of water transparency.

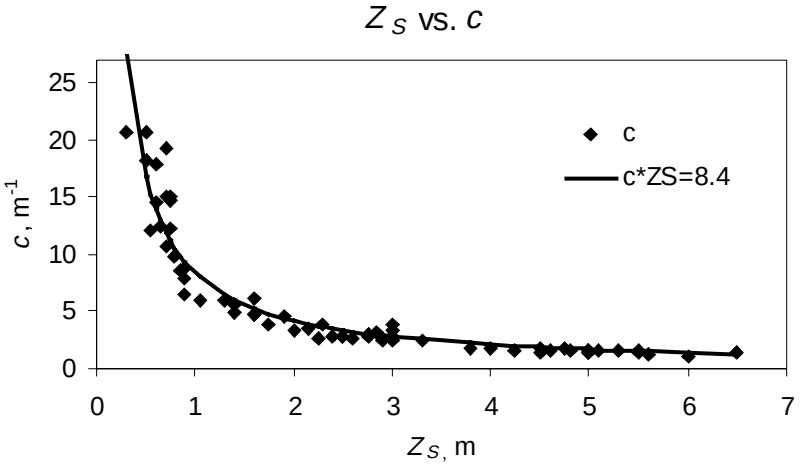

Figure 11. The correlative relationship between the total beam attenuation coefficient, *c* in the PAR region and the Secchi depth using all data from 1997-2000.

The next relationship that was studied is between the Secchi depth and the diffuse attenuation coefficient K_d. The empirical observation has been made that the Secchi depth is approximately inversely proportional to the attenuation for downwelling irradiance. Holmes' (1971) relation $K_d = 1.44/Z_S$ is widely used. Højerslev (1986) pointed out that this value is too small. We compared the values of K_d and Z_S in 100 cases during six years and found $K_d = 2.6/Z_S$ with $R^2 = 0.74$.

It has been concluded that the reciprocal of Z_S is proportional to $(c+K_d)$. On theoretical grounds Tyler (1968) arrived at the relation $(c+K_d)=8.69/Z_S$, as referenced in Kirk (1994). Holmes obtained from measurements $(c+K_d)=9.42/Z_S$. Our result was $c+K_d=11.2/Z_S$ with $R^2=0.93$. In natural waters *c* is substantially greater than K_d. In this work the relation was found to be $c = 2.81K_d$ ($R^2=0.80$), hence Zs is determined more by *c* than by K_d and also the correlation between Z_S and *c* was better than between Z_S and K_d. It has been concluded that the primary function of the Secchi depth is to provide a simple visual index of water clarity in terms of Z_S or $(c+K_d)$ and it can be referred to as the contrast attenuation coefficient (Kirk, 1994).

7.2.2 A spectral model connecting *c* and K_d

A spectral model connecting *c* and K_d (explained in detail in papers II and III) is briefly described here. The relationships between the numerical values and spectral distributions of the downward irradiance attenuation coefficient and the beam attenuation coefficient were investigated. Measurement data obtained in 1994-95 and 1997-98 for 18 Finnish and Estonian lakes were used. Formulae connecting the values of the downward irradiance attenuation coefficient, absorption coefficient, and the scattering coefficient for different illumination conditions were used to determine the spectra of $K_d(\lambda)$ from measured $c(\lambda)$ spectra. Correlation analysis of the model's results gave the relationship $K_{dm}=1.0023K_{dc}$

(measured and calculated K_d) with a number points 885, the correlation coefficient 0.961 and the standard deviation of K_d 0.55 m^{-1}.

The first model was developed in 1996 and the results published in paper II in 1997. As known, connections between $c(\lambda)$and $K_d(\lambda)$ are described by Kirk's (1984, 1989) formulae:

$$K_d(avg) = \frac{1}{\mu_0}\left[(c-b)^2 + (0.425\mu_0 - 0.190)(c-b)b\right]^{1/2} \quad (28)$$

for clear sky and

$$K_d(avg) = 1.168\left[(c-b)^2 + 0.162(c-b)b\right]^{1/2} \quad (29)$$

for overcast conditions.

Here K_d(avg) is the vertical average value for the euphotic zone, b is the scattering coefficient, and μ_0 is the cosine of the refracted direct solar beam just beneath the water surface. As seen, also the values of scattering coefficient, b are needed. The relationships between c and b were described by the following way: b(580nm)= 0.8c(580nm) and the spectrum of $b(\lambda)$ was calculated relying on b(580) using either linear or power function of λ (paper II).

However, the constant ratio b(580)/c(580)=0.8 is only an approximate result and valid for limited number of water bodies. We wanted to improve the model to be valid for a wide range of water bodies, especially for waters dominated by yellow substance, using data from 1994-95 and 1997-98 in 9 Estonian and 9 Finnish lakes. The spectra of two characteristics were available for our investigations (in paper III): (1) beam attenuation coefficient estimated from water samples in the laboratory by spectrophotometer *Hitachi* U1000; (2) diffuse attenuation coefficient measured in situ by underwater spectrometer LI-1800UW.

Here it should be noted that the measurement of beam attenuation coefficient is a complicated task for any type of spectrophotometer. The definition of the beam attenuation coefficient requires that the instrumentation used to measure it rejects all scattered light. However, in reality all transmissometers accept some portion of the small-angle forward scattered light. The measured transmittance then exceeds the theoretical value and the attenuation coefficient determined from the measured transmittance is less than the true value (difference is 4-10 % of the total scattering for *Sea-Tech* transsmissometers, more for Hitachi). This upper limit (0.1) was used in this model work for the Hitachi data.

The results by *Hitachi* U1000 give us the difference between the attenuation coefficient of the water under investigation and that of distilled water. By treating the water samples the value $c^*(\lambda)$ is obtained:

$$c^*(\lambda) = c(\lambda) - Fb(\lambda) - c_d(\lambda) \quad (30)$$

where c is the real beam attenuation coefficient, Fb is the contribution of the small-angle forward scattering to the measured radiation (F=0.1 in this model test), and c_d is the attenuation coefficient of distilled water (all in m^{-1}).

We tried to find out the algorithms, which lead to most successful correspondence between the calculated and measured spectra of K_{dc} and K_{dm}, respectively. The algorithms chosen by us for determining the value of $A=b(580)/c(580)$ and the method for correction of the Hitachi results are described in more detail in paper III. The basic idea in

determining A was to define a coefficient A^*_1, that describes the relative difference between measured beam attenuation coefficients of unfiltered and filtered water. As known, this difference is a good characteristic showing the influence of the particulate matter on the light attenuation. The variation of A was found to be in the range of 0.30-0.89 after applying the algorithms to calculate it to the lakes presented in Table 1 in paper III. The low values of A belong to the clear water lakes (Päijänne, Paukjärv, Puujärvi) as well as to brown-water Lake Pääjärvi (in this lake due to high content of yellow substance the absorption is bigger or comparable with scattering even at 580 nm).

The final values of $b(580)$ and $c(580)$ were found through an iteration of the equations

$$b_n(580)=Ac_{n-1}(580),$$
$$c_n(580)=c_{n-1}(580)+0.1\,b_n(580), \tag{31}$$

starting with n=1 to calculate b_1, then use that value to obtain c_1 and so forth, proceeding until n=10. The starting value $c_0(580)$ is the value of $c_m(\lambda)$ obtained from Hitachi measurements for 580 nm. After 5-7 steps the values of $c(580)$ and $b(580)$ were almost stabilized. The final result was $b(580)=Ac(580)$, where $b(580)$ and $c(580)$ are corrected values of scattering and beam attenuation coefficients.

For describing the spectral distribution of the scattering coefficient we used the power law

$$b(\lambda) = b(580)\left(\frac{580}{\lambda}\right)^{n_b} \tag{32}$$

where n_b=0.8. This value was chosen relying on the results of spectral distribution of scattering coefficient measured by ac-9 in 12 Finnish and Estonian lakes (paper IV and later confirmed in paper VIII). Using the values of $b(\lambda)$ the corrected spectra of $c(\lambda)$ were determined by the following way: $c=c_0+0.1b$. Relying on the spectra of c and b determined by our model the spectra of diffuse attenuation coefficient were calculated by Eq.(28) or (29).

Some examples of the results can be seen in Figs. 1-3 in paper III. The lakes chosen for these figures are rather different in their transparency and content of optically active substances (Table 1 in paper III). The highest absolute differences between K_{dc} and K_{dm} occurred in case of a turbid lake Vörtsjärv and also at wavelengths 400-420 in a brown lake Pääjärvi. As explained below the scattering correction factor F (in Eq. 30) used in these model calculations was too small, but in those cases of Vörtsjärv and Pääjärvi mentioned above, it happened to be closer to the actually measured ones. This may be an explanation to the higher differences between K_{dc} and K_{dm} when using these model parameters. However, the relative errors rarely exceeded 30 % even in the most turbid lakes.

After this model development we had a possibility to use the ac-9 instrument. Based on the ac-9 data the following observations and calculations were made. The average attenuation coefficient, c(412-715nm) (ac-9) was compared to the average attenuation coefficient c^*(400-700) (Hitachi). The mean value for c^*/c was found to be 0.76, measured in 75 cases. Eq. (30) was tested using the measured values of c, b, c_d and c^*. The correction factor F, due to the contribution of the small-angle forward scattering to the measured radiation in Hitachi, was found to be 0.27 on the average. This value contains uncertainties due to measurement errors, but it indicates that the error due to scattering in Hitachi spectrophotometer is larger than anticipated. The value of F was smaller for brown waters. Also the coefficient $A=b(555)/c(555)$ was calculated using ac-9 data. The values

found were between 0.52-0.98, with the mean value being 0.81. Also these values were larger than the values derived by the model algorithm described above, but the difference was not essential.

Although the measured values of F were clearly larger than used in the model the overall agreement between K_{dc} and K_{dm} was good when using the parameters mentioned above and Eqs. (28)-(29). This may be due to a balancing effect between the parameters used in this model and the general coefficients used in Eqs. (28)-(29). It was later found that the coefficients in those equations were somewhat different for our waters (see chapter 7.2.4. and paper VII). Nevertheless, the overall conclusion is that it is possible to build a model to derive the values of diffuse attenuation coefficient from spectral beam attenuation coefficient measured from water samples. Possibly, to minimize errors, it may be good to group the lakes according to their dominant substance in the water and then obtain different algorithms for each group. It may also be worth while to test the algorithms with different values of F and different coefficients in Eqs. (28)-(29).

7.2.3 A relation between $K_{d,PAR}$ and $K_d(\lambda)$

The following describes the relation between the broadband attenuation coefficient $K_{d,PAR}$ and the spectral attenuation coefficient $K_d(\lambda)$. We found an analytical expression for lakes under investigation taking the value of $K_d(490)$ as a reference value. From the plot of all K_d values for every 5 nm from 400 to 800 nm against the corresponding value of $K_d(490)$, we found a strong linear relationship between these two variables. The slope parameter $M(\lambda)$ and the intercept $I(\lambda)$ for all 81 wavelengths were based on fitting the following linear equation by the least squares technique:

$$K_d(\lambda) = I(\lambda) + M(\lambda)K_d(490). \quad (33)$$

The parameters M and I can be found in Table 3 in paper V and $K_d(490)$ given by the formula:

$$K_d(490)=1.76\ K_{d,PAR} + 0.07(\pm 0.36). \quad (34)$$

By this method the whole spectrum of K_d can be calculated. An unknown value of K_d at the wavelength λ_2 is calculable from a known $K_d(\lambda_1)$ by applying Eq.(33) twice:

$$K_d(\lambda_2)=I(\lambda_2)+[\ K_d(\lambda_1)- I(\lambda_1))]M(\lambda_2)/M(\lambda_1). \quad (35)$$

This is useful for determining some missing K_d values. When comparing the results obtained from Eq.(33) and measured values of K_d a satisfactory correspondence was found with only a few exceptions. The correspondence was good if $K_d(490)$ values ranged from 0.6 to 5.6 m^{-1}. Relative error was the highest around 680 nm being ~10% over the whole spectrum. The value of $K_d(490)$ could be used as a classification index for clear and moderately turbid waters in Boreal region. However, the waters with a very high content of yellow substance or extremely turbid ones need a more complicated model.

7.2.4 Relations between K_d and a and b

The relation that was studied most during this work was between K_d and the inherent optical properties absorption, a and scattering, b. These relations can be used in light field models and indirectly in bio-optical remote sensing. As mentioned if one is able to

calculate K_d or R from absorption and scattering it is possible to connect the AOP's and the concentrations of the OAS. The starting point was to test the validity of a formula relating K_d to a and b developed by Kirk (1984) (Eqs. (28)-(29)) and thereafter modify formulas to fit with the measured data. The different formulas did not show considerable variation using our data set, thus to start with, Eq.(29) for totally overcast conditions was chosen.

All the data with simultaneous irradiance and absorption and scattering measurements (102 cases) were compared to find the relations between K_d and a and b. K_d was calculated from Li-1800UW irradiance data and a and b were measured by the ac-9. All spectra of measured and calculated K_d were initially plotted in a same graph for comparison. Kirk's formula that was used as a starting point is of the form:

$$K_d = A(Ba^2 + Cab)^{\frac{1}{2}} \tag{36}$$

The coefficient A was kept constant (1.2) and B and C were then optimized to fit and the best fit compared with the measured spectra was chosen for each case.

The results of the first test are shown using four classification procedures in the Tables 2-4. Two somewhat qualitative classifications have been used. The first in Table 2 is a simple one dividing the water types into three categories (clear, moderate/turbid, brown). The second classification in Table 3 is based on the concentrations of the optically active substances and apparent optical properties (Reinart, 2000) using five different water types (**C**lear, **M**oderate, **T**urbid, **V**ery turbid, **B**rown) with more complex definition of each class. The variation is significant, but even if one chooses a mean value for all the data together (A = 1.2, B = 0.88, C = 0.45), the improvement is considerable compared to the original Kirk's formula (A=1.17, B=1.0, C=0.16). Some features could be found more prominently in the first and more simple classification. A common feature for both classifications was that for brown waters the value of C was distinctly larger than the average. One explanation for this may be the type of the studied waters (many of them are brownish), since in cases of brown waters the value of C is up to twice this average. The brown waters were examined more closely and it was found, that even though the ratio of scattering to absorption was small, the scattering was substantially larger (b_{ave}= 1.9 m^{-1}) than in clear waters (b_{ave}= 0.8 m^{-1}) due mostly to chlorophyll. In these brown waters the impact of scattering on K_d is enhanced by its significant contribution to the average cosine (of the zenith angle) of the downwelling photons. Therefore the value of the coefficient C in Eq. (36) is so large. Another explanation may be the choice of the volume scattering function used in Kirk's studies. He has stated that the shape of the volume scattering function affects C and it could be found from his study that in waters with higher backscattering the coefficient contributing to scattering should be larger. This may also be the case in our turbid and brownish waters.

Two more simple and quantitative classifications were made. The data was divided into three classes using the total absorption, scattering and attenuation in the PAR region. The results can be seen in Table 4.

Table 2. Results of the first test to derive the coefficients B and C used in Eq.(36) using three classes.

Lake type	A	B	C
Clear	1.2	0.99	0.29
Moderate/**T**urbid	1.2	0.77	0.46
Brown	1.2	0.86	0.78
Average of all 102 cases	1.2	0.88	0.45

Table 3. Results of the first test to derive the coefficients B and C used in Eq.(36) using five classes

Lake type	A	B	C
Clear	1.2	0.97	0.24
Moderate	1.2	0.93	0.43
Turbid	1.2	0.72	0.52
Very turbid	1.2	0.91	0.41
Brown	1.2	0.80	0.97
Average of all 102 cases	1.2	0.88	0.45

Table 4. Results of the first test to derive the coefficients B and C used in Eq.(36) classified by *a*, *b* and *c*.

c	A	B	C
0-1.99	1.2	0.94	0.28
2.0-5.99	1.2	0.97	0.42
6.0-25	1.2	0.73	0.55
b/a	A	B	C
0-0.99	1.2	0.91	0.61
1.0-2.69	1.2	0.96	0.34
2.7-10.0	1.2	0.78	0.44

A second test was made to examine a simple relationship between K_d and a and b. Based on earlier studies on this subject (Maffione, 1998; Maffione and Jaffe, 1995) the following relationship was chosen:

$$K_d(\lambda) = \mathrm{A}a(\lambda) + \mathrm{B}b(\lambda), \tag{37}$$

After some preliminary tests we started with the initial values of A = 1.2 and B = 0.2. The procedure was identical with the previous test using the Kirk's formula. The coefficients A and B were alternated to fit with the measured spectra and the best fit was chosen for each case (102 cases). The results can be seen in tables 5-6, with similar classifications of the water types as in the first test (the second classification with five water types was omitted, since it did not give any additional information).

The results (A=1.21, B=0.19) show in the second test, using these classifications, that the value of A is larger than the original value (1.0) found by several authors and the value for B is closer to the original (0.15). The clear exception again is the brown water class, where B is almost twice the average (0.38). The explanation is the same as for coefficient C in Test 1 for brown waters. The situation is the same in all three classifications. On the other hand the value for A was larger in almost every case and it was more stable. This second formula has a simple form and thus convenient to use and it is justified to use the average coefficients 1.2 and 0.2 for other water types than brown waters. The reason for the coefficient A contributing to the effect of absorption being larger than found earlier is difficult to explain by other reasons than the water types in our studies. The scattering values are generally quite high (total scattering varying between 0.53-19.19 m^{-1}, average being 4.48 m^{-1}) and the more scattering, the greater the influence of absorption on K_d.

Table 5. Results of the second test to derive the coefficients A and B used in Eq.(37) using three classes.

Lake type	A	B
Clear	1.21	0.14
Moderate/Turbid	1.21	0.18
Brown	1.15	0.38
Average of all 102 cases	1.21	0.19

Table 6. Results of the second test to derive the coefficients A and B used in Eq.(37) classified by *a*, *b* and *c*.

c	A	B
0-1.99	1.18	0.13
2.0-5.99	1.19	0.20
6.0-25	1.22	0.20
b/a	A	B
0-0.99	1.17	0.29
1.0-2.69	1.20	0.16
2.7-10.0	1.22	0.16

Regression formulas between *K* and *a* and *b* were calculated using integrated values for them in the PAR region (actually in the region 412 – 715 nm, due to the ac-9 wavelengths). The following results with good correlations ($R^2 > 0.85$) were obtained:

$$K_{d,PAR} = 1.17(\pm 0.06)a_{PAR} + 0.13(\pm 0.02)b_{PAR}, \qquad n=64, R^2=0.88, p<6\cdot 10^{-11} \quad (38)$$

$$K_{d,PAR} = 1.2\left[0.70(\pm 0.08)a_{PAR}{}^2 + 0.38(\pm 0.05)a_{PAR}b_{PAR}\right]^{\frac{1}{2}}, \quad n=64, R^2=0.88, p<2\cdot 10^{-11} \quad (39)$$

$$K_{d,PAR} = \frac{1}{\mu_0}\left[0.66(\pm 0.09)a_{PAR}{}^2 + 0.43(\pm 0.06)\mu_0 a_{PAR}b_{PAR}\right]^{\frac{1}{2}}, n=64, R^2=0.86, p<4\cdot 10^{-10} \quad (40)$$

The regression results above support the results obtained by comparing calculated and measured K_d spectra, and adjusting the coefficients in the formulas to obtain the best match between calculated and measured K_d. The average values obtained in this manner are quite close to the values of the coefficients in the equations above. The effect of the solar altitude, as μ_0, was taken into account in the last calculation, but it did not improve the regression.

A useful approach to improve the equations between K_d and *a* and *b* could be to introduce a further correction term, which could take into account the type of the water. If that would work properly then the equation could be valid for all water types. Another improvement could be to find direct relations between the coefficients A, B or C and the inherent optical properties *a* and *b* instead of classifying waters into different types.

7.2.5 Scattering and backscattering in Nordic waters

7.2.5.1 Scattering

The spectral distribution of the total scattering, *b* obtained from the ac-9 data was investigated. Different authors have noted that the spectral distribution of *b* is influenced by the turbidity of the water, however this kind of studies are rare and have not been undertaken for data from Nordic waters. The spectral dependence can be explained by a power law $b = b_0(\lambda_0/\lambda)^{nb}$. Jerlov and Steemann Nielsen (1974) shows that the wavelength dependence of *b* becomes weaker with increasing turbidity and the value of the exponent n_b for Baltic waters is close to zero. Bukata et al. (1979) found *b* to be spectrally invariant in Lake Ontario, as does Phillips and Kirk (1984) in Australian waters. Gould and Arnone (1998) show decreasing *b* with wavelength the exponent n_b being about 1.05. Kirk (1994) mentions in his book that there is evidence that *b* varies approximately with λ^{-1}. Halturin et al. (1983) show that for the clearest ocean water n_b is about 1.22. Thus, most of these previous results indicate that the n_b is decreasing with increasing turbidity.

The largest n_b in our results was 2.42 and the smallest was 0.13, the mean value being 0.78. Remarkably there was only a poor correlation between the average scattering coefficient *b* (and also the beam attenuation coefficient *c*) and the spectral wavelength dependency n_b (n=98, $R^2 = 0.14$, $p<1.5\cdot10^{-4}$). This suggests that in our data as a whole turbidity does not affect the wavelength dependence of *b*. During the early summer (May/June) we found a clearly larger wavelength dependence in scattering than in August (Fig. 12). The average n_b in May/June was 0.9 and in August 0.66, while the average *b* remained nearly the same, about 4.5, both times. In some cases the difference was really large in a certain lake even with comparable turbidity values, e.g. in lake Tuusulanjärvi (a eutrophic turbid lake) the average May and August values for n_b were 1.91 and 0.55, respectively. Also the correlation between n_b and *b* was positive and better in May/June data (n=46, $R^2 = 0.37$, $p<7.6\cdot10^{-6}$). The best correlation was between n_b and *b* measured in May (n=30, $R^2 = 0.78$, $p<1.39\cdot10^{-10}$) (Fig.13). The correlation between the average total scattering and the concentration of total suspended matter was $Cs = 1.3\ b$, (n=82, $R^2 = 0.72$, $p<2.22\cdot10^{-37}$).

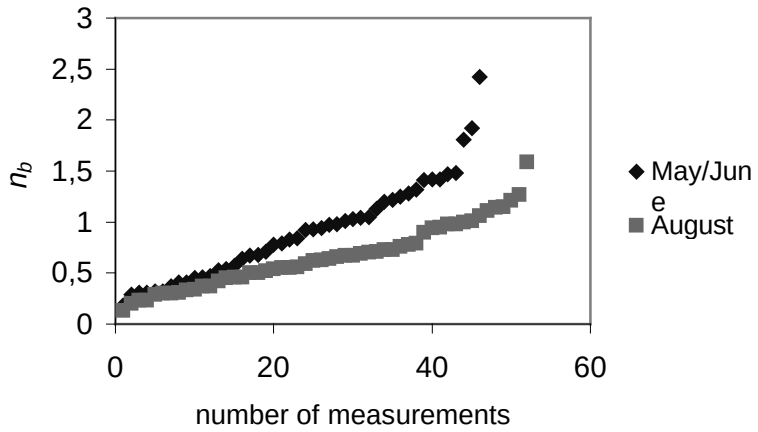

Figure 12. The wavelength dependence n_b of scattering, *b* in May/June data and August data in Finnish and Estonian waters during 1997-2000.

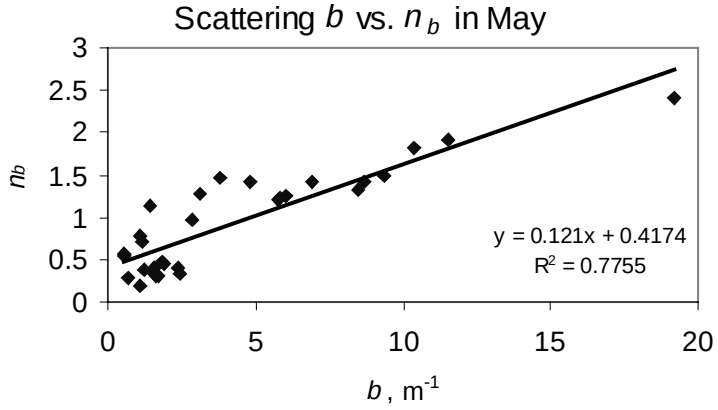

Figure 13. The correlation between wavelength dependence, n_b and b measured in May in Finnish waters during 1997-2000.

These results show that the correlation between the average turbidity and the wavelength dependence of b was weak, except in May when the correlation was also positive, meaning that turbidity increases the wavelength dependence of b. This contradicts the results found by the authors mentioned in the beginning of this chapter. The question of why the wavelength dependence of scattering is larger in spring than in late summer can be explained by the size and type of the particles in the water. In the spring after the snowmelt the water contains relatively more small mineral particles from the river runoff and the general spring runoff. In August the amount of algae (larger colloids) is larger. Another factor is that living cells contribute to the backscattering much less than mineral or detrital particles and that forward scattering is virtually independent of wavelength (Kirk, 1994; Jerlov, 1968). Hence smaller mineral particles contribute more to backscattering, which is more wavelength dependent than forward scattering. The results of our bio-optical determinations of the concentrations of the OAS support the fact that in August when the n_b was smaller in the turbid lakes the concentration of chlorophyll-a was also large.

If one intends to find a spectrum for total scattering using a single value for scattering, the time of the year is crucial and also the type of water, but as a rule of thumb b varies approximately with $\lambda^{-0.8}$ (or λ^{-1}).

7.2.5.2 Backscattering

The backscattering probability, $\tilde{b}_b = B = b_b/b$, and the coefficient C in Eq.(16) were studied by different methods (see paper VIII). It seems that C is getting larger when moving towards more turbid waters starting from class **B**, except for class **V** (Table 1 in paper VIII). This phenomenon is the clearest in case of using a common $\tilde{b}_b$ value (0.019) for all cases. The result appears to be clear, but the very turbid water case (**V**) needs further explanation. It seems that the value of $\tilde{b}_b$ used to reach the C values have been too large in the **V** class. There is a reason to believe (explained later), that the backscattering probabilities for very turbid waters in our case were in reality smaller than the ones chosen here or the widely used value obtained by Petzold (0.019) using data from the San Diego harbor (Kirk, 1994). This study indicates, that the value of C in the Eq.(16) is changing with the water type as well as with the solar elevation and it is slightly smaller than the value proposed by Kirk (1984) in Eq. (17).

The results of the backscattering probability study show that $\tilde{b}_b$ is increasing when moving towards more turbid waters starting from class **B**, except in class **V** in a similar fashion with *C*. The size distribution and the type of scattering particles were thought to be crucial also for the behavior of $\tilde{b}_b$ (the size distribution of particles was measured in one experiment, the result of which supports the overall conclusions). Moving from brown waters towards more turbid waters backscattering increases due to the increase in the amount of inorganic particles, which scatter at larger angles than organic particles. The same applies to reflectance (Eq. (16)), since it is controlled by backscattering when there is substantial amounts of inorganic particles present. Smaller particles contribute more to large angle scattering than larger particles. Nevertheless in very turbid class the concentration of chlorophyll and organic particles is so large (> 40 mg m^{-3} in our case) that they dominate the scattering process where forward scattering is enhanced. This can explain why the backscattering probability, $\tilde{b}_b$ in the class **V** is so small. The average value for all calculated cases was 0.015, which is smaller than the value found by Petzold (0.019). Kirk (1994) states that above a certain level of turbidity, such that particle scattering is dominant at all angles, the normalized volume scattering function is not expected to alter its shape with increasing turbidity. This is why the value 0.019 may be applicable to the majority of natural waters other than the very clear oceanic ones. However, when the scattering is dominated by organic particles with a low refractive index a different shape of volume scattering function might be appropriate. Our results support this at least in the very turbid water case, but why is the value for $\tilde{b}_b$ in e.g. the clear water case so much smaller than Petzold's value? It may be that even our 'clear' lakes contain a relatively large amount of chlorophyll to diminish the backscattering probability or the value for the coefficient *C*. In the turbid water case (**T**) the inorganic particles are dominating giving the value for $\tilde{b}_b$ about 0.02.

By studying the values of $\tilde{b}_b$ measured in Sweden the following observations were made. The average values were 0.014 in varying waters and 0.019 in lake Vänern (Table 7). The difference due to the time of the year was clear. In lake Erken the value of $\tilde{b}_b$ was about 0.010 in May and 0.017 in October. This and the fact that the total absorption was clearly higher in May indicate that there was chlorophyll present. Another notable feature was that the value of $\tilde{b}_b$ could change so much at a single site i.e. $\tilde{b}_b$ was 0.015 at the depth of 0.5 m and 0.018 at the depth of 4.0 m and 0.019 at the depth of 0.5 m again the following day. Hence it is difficult to find a reliable value for $\tilde{b}_b$ that represents a water type or even a single lake. Still taking into account the time of the year and the general conditions of the water area under study, it is possible to find an estimate for $\tilde{b}_b$.

Table 7. Values of n_B, describing the wavelength dependence of backscattering probability $\tilde{b}_b$, $\tilde{b}_b$ itself and the total scattering, b measured in Sweden 1998/1999 and 2001.

1998/1999 Lakes and sea	n_B	$\tilde{b}_b$	b	2001 Vänern	n_B	$\tilde{b}_b$	b
Erken 131098 0.5 m	0.46	0.015	1.54	1	0.72	0.022	0.90
Erken 1310 4.0 m	0.23	0.018	1.36	1000	0.78	0.018	0.85
Erken 141098	0.58	0.019	1.09	2000	0.82	0.018	0.87
Harkö 151098	0.58	0.016	3.07	3000	0.69	0.016	1.01
Käringö 151098	0.74	0.012	0.56	4000	0.59	0.016	1.60
Erken 070599	0.84	0.010	1.22	5000	0.52	0.020	2.37
Harkö 130599	0.76	0.015	3.07	6000	0.51	0.020	2.82
Lidön 130599	0.85	0.011	0.74	7000	0.48	0.022	2.77
Average	0.63	0.014	1.58	8000	0.56	0.017	2.48
				9000	0.6	0.017	1.85
				10000	0.77	0.019	1.18
				Average	0.63	0.019	1.70

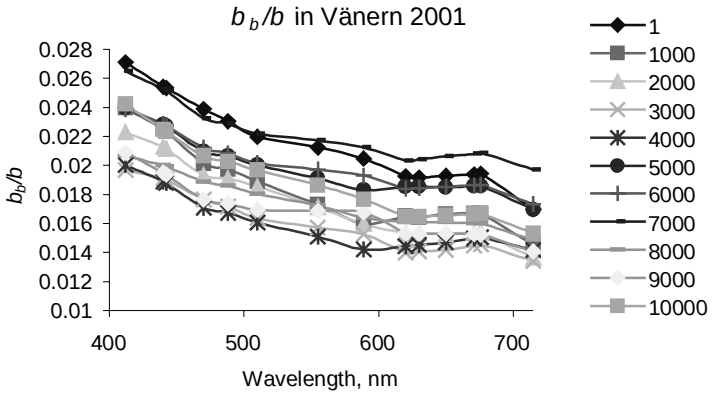

Figure 14. Examples of the spectra of backscattering probability, $\tilde{b}_b$ calculated from data measured in lake Vänern in July 2001. The legend numbers refer to distance along the transect line.

The wavelength dependence of both b_b and $\tilde{b}_b$ expressed similarly with the case of total scattering shown earlier in this study, i.e. $\tilde{b}_b = \tilde{b}_{b,0}(\lambda_0/\lambda)^{nB}$ were also studied. The results can be seen in Table 7 and some examples of the $\tilde{b}_b$ spectra in Fig.14. The average values of nb_b in 1998 and 1999 in variable waters was 1.31 and in Vänern, 2001 1.61. The values of n_B in 1998, 1999 cases were also more variable than in Vänern, 2001, but the average value was 0.63 in both cases. One clear feature can be seen in the results, the value of n_B (and nb_b) was larger in spring than in autumn, i.e. backscattering was more wavelength dependent (and smaller) in May than in October. Another interesting fact is that especially in 2001 the value of n_B correlates well in a negative direction with the value of total b (and b_b) (n=11, R^2=0.88, $p<2.15\cdot10^{-5}$). The larger the scattering (and backscattering) the smaller the wavelength dependence of $\tilde{b}_b$, which is opposite to the behavior of b seen earlier in this study. In fact this data shows also positive correlation between n_b and b. The results of the backscattering probability studies are interesting and further studies and experiments of simultaneous measurements of b_b, R, a and b will be performed. These studies are valuable especially for remote sensing hyperspectral modeling.

7.3 Modeling

Remote sensing of natural waters can basically be made through two different approaches or through a combination of the two; empirically or semi-analytically. In the empirical approach, remote sensing data is related by regression analysis to in-situ measurements of water quality parameters. This approach needs extensive field work and logistics. The advantage of this method is that it can be very accurate during one campaign in a limited area. Empirical methods and spectral band ratios and their combinations are widely used to interpret remote sensing data. Nevertheless, remote sensing algorithms often have a local and seasonal character. Algorithms developed for certain water body cannot be used everywhere and seasonal coefficients may be needed to use an algorithm the year round.

To overcome the reliance on statistical methods for the interpretation of remote sensing data a hyperspectral model was developed for simulation of watercolor spectra above and beneath the water surface (Arst & Kutser, 1994; Kutser, 1997; Kutser et al. 1997; Kutser et al., 1998d.) This was done to test the possibility of estimating chlorophyll-a, dissolved and total organic carbon and suspended matter concentrations in the turbid Nordic waters. A prototype of the model was based on data available in literature (mainly from clear oceanic waters). Our database was insufficient during the first years to be able to improve the model when it became clear that the model with oceanic water parameters could not describe the reflectance spectra of waters with high yellow substance content and turbidity. After collecting new data during 1994-1998, a hyperspectral model was improved for simulation of reflectance spectra above and beneath the water surface (described in paper VI). The database for the last version of the model has been collected during 1997-2001 and the concentration was on the underwater reflectance (paper VIII). Semi-analytical models have proven to be suitable for interpreting remote sensing measurements if their parameterization is performed with care. The basics of the model and the latest improvements and simplifications are presented here.

7.3.1 Basics of the model

The basic equation of this model is Eq.(16) developed by Gordon et al. (1975) in their Monte Carlo study relating the irradiance reflectance just beneath the water surface with a polynomial function of absorption and backscattering coefficients, where C is a function of solar altitude (Eq.(17)). The variability range of $C(\mu_0)$ in our case is between 0.40 and 0.50. (latitude 58^oN to 67^oN; solar zenith angle 60^o or more). It is obvious that an expression like Eq.(16) contains assumptions regarding the light field and the average shape of the volume scattering function. Taking into account the refraction at the water-air interface, Eq.(20) can be used.

We assume, as mentioned, that there are three optically active components in the water: phytoplankton, yellow substance and non-chlorophyllous suspended matter and the total absorption and scattering coefficients are additive over the constituents of the medium by the definition of inherent optical properties. Under these conditions the total spectral absorption coefficient of the water, $a(\lambda)$, is described by Eq.(21) and the total spectral backscattering coefficient $b_b(\lambda)$ is described by Eq.(22).

7.3.2 Model parameters

Absorption and backscattering due to yellow substance and suspended matter are often expressed through empirical functions of C_{Chl} (Gordon et al., 1988; Lee et al., 1994). That is acceptable in oceanic waters, but not in coastal and inland waters where concentrations of optically active substances are not in correlation with chlorophyll-a concentration. It would be preferable to use spectra of specific absorption and scattering coefficients measured in the water body under investigation. Unfortunately this kind of data is unavailable in most cases and variability of the parameters is very high, sometimes varying over two-three orders of magnitude.

The semi-analytical model developed here uses concentrations of the three optically active substances as input and gives estimates of irradiance reflectance as the output. When used in a reverse way (inverse modeling) the concentrations of the OAS are achieved. These concentrations are linked, as mentioned, to the two inherent optical properties of the water, the absorption, a and the backscattering, b_b. The parameterization of this model is based on *in situ* measurements and laboratory analysis of both the concentrations and the inherent optical properties.

The values of absorption and scattering coefficients of pure water, $a_w(\lambda)$ and $b_w(\lambda)$, were taken from Smith and Baker (1981). The spectral chlorophyll-specific absorption coefficient of phytoplankton is calculated by Eq.(19). The values for A and B used in the latest study were estimated by Strömbeck (2001) based on laboratory measurements of a^*_{Ph}. For each measured a^*_{Ph} spectrum, regressions were used to define power functions (Eq.(19)) and coefficients $A(\lambda)$ and $B(\lambda)$. They were tested in the model and found to work better in our test sites than Bricaud's values. The absorption by yellow substance is calculated by Eq.(18).

Our data set enables us to estimate the specific absorption coefficient of non-chlorophyllous suspended matter using the assumptions described above. According to Eq.(21) the specific absorption coefficient of the suspended matter can be calculated with the formula:

$$a^*_{SM}(\lambda) = \frac{a(\lambda) - a_Y(\lambda) - a_w(\lambda) - a^*_{Ph}(\lambda)C_{Chl}}{C_{SM}}. \quad (41)$$

The total absorption coefficient $a(\lambda)$ was measured in situ with ac-9 and interpolated to spectra of 5 nm wavelength intervals between 400-700 nm. $a_Y(\lambda)$, C_{Chl} and C_S (dry weight of all particles) were determined from water samples and C_{SM} is calculated using $C_{SM}=C_S-0.07C_{Chl}$ (Hoogenboom and Dekker (1997) as referenced in paper VI). The $a^*_{Ph}(\lambda)$ is calculated as described in Eq.(19) in chapter 4.3..

In Eq.(22) for backscattering there are four unknown parameters: specific scattering coefficients of phytoplankton and non-chlorophyllous particles ($b^*_{Ph}(\lambda)$ and $b^*_{SM}(\lambda)$) as well as the backscattering probabilities ($b_{b,Ph}/b_{Ph}(\lambda)$ and $b_{b,SM}/b_{SM}(\lambda)$). In the latest study after some testing a more simple equation was chosen for backscattering i.e.

$$b_b(\lambda) = 0.5b_w(\lambda) + b^*_{b,S}(\lambda)C_S, \quad (42)$$

where S stands for total suspended matter including phytoplankton. Thus there are only two unknown parameters, $b^*_S(\lambda)$ and $b_{b,S}/b_S(\lambda)=\tilde{b}_{b,S}$. This simplifies the model and it was found that separately including the effects of phytoplankton on backscattering did not improve the results, rather the opposite. One reason for this is that there are very little information on specific absorption, scattering and backscattering coefficients of different

algae species available and there was no data available on the optical properties of algae species present in the waters under this investigation. Forward modeling, that uses concentrations of the three optically active substances as input and gives estimates of irradiance reflectance as the output, was carried out in three steps. The first step was to search for $a^*_{SM}(\lambda)$. The second step was to search for parameters necessary for a calculation of the total backscattering coefficient. Thirdly we need also backscattering probability of particles.

7.3.3 Model Results

After calculating the spectra of $a^*_{SM}(\lambda)$ they were plotted and they seemed to decrease exponentially with increasing wavelength. The usage of Eq. (46) produced some uneven shapes to the spectra of $a^*_{SM}(\lambda)$ due to the shape of the $a^*_{Ph}(\lambda)$ spectra. However $a^*_{SM}(\lambda)$ was described using two parameters $a^*_{SM}(400)$ and the slope of an exponential curve (S_{SM}) analogous to those in Eq. (18). $a^*_{SM}(400)$ and S_{SM} were derived by fitting an exponential trend line for the calculated $a^*_{SM}(\lambda)$ spectra.

The unknown parameters for a calculation of the backscattering coefficient, after making assumptions described above, were specific scattering coefficient of all particles, $b^*_S(400)$, and the exponent n_S for calculating $b^*_S(\lambda)$. It was tested that a power function $b^*_S(\lambda) = b^*_S(400)(400/\lambda)^{nS}$ describes best the wavelength dependence of b^*_S . The scattering coefficient was calculated using the following formula:

$$b_S^*(\lambda) = \frac{b(\lambda) - b_w(\lambda)}{C_S}, \tag{43}$$

where $b(\lambda)$ was obtained from ac-9 measurements and b_w was taken from Smith and Baker (1981). The $b^*_S(400)$ and the exponent n_S were estimated from the calculated spectra of $b^*_S(\lambda)$. Another choice for n is to use the average value of 0.8 calculated for total scattering.

We need also backscattering probability of particles, $\tilde{b}_{b,S}=b_{b,S}/b_S$ to model irradiance reflectance spectra. This parameter can be calculated using Eqs. (44)-(45). If

$$b_{b,S} = b_b - 0.5b_w \tag{44}$$

it follows, that

$$\tilde{b}_{b,S} = \frac{\tilde{b}_b b(\lambda) - 0.5b_w(\lambda)}{b(\lambda) - b_w(\lambda)}. \tag{45}$$

where total $\tilde{b}_b=b_b/b$ can be estimated from Eq.(16) using reflectance spectrum calculated from LI-1800UW data and absorption and scattering spectra measured by ac-9. The backscattering probability of particles calculated like this varied more than an order of magnitude. After dividing the probabilities with C_S we got a power function that describes the dependence of the probability on the concentration of all particles. Nevertheless this dependence was not well correlated ($R^2<0.5$), so another method was introduced. The backscattering probabilities for suspended matter (Eq.(45)) were compared to the total backscattering coefficients from Eq.(16) and the following average relation was found $\tilde{b}_{b,S}= 0.93\tilde{b}_b$. The average backscattering coefficients calculated for five water types (Table 1 in paper VIII) and the above relation were used to give a representative value for $\tilde{b}_{b,S}$.

The model results using these average values for $\tilde{b}_{b,S}$ were better than using the relationship between C_S and $\tilde{b}_{b,S}$.

The use of power functions instead of average values of $a^*_{SM}(\lambda)$ and $b^*_{b,S}(\lambda)$ improved significantly the fitting of measured and simulated spectra. Also regression formulae for model parameters ($a^*_{SM}(400)$, S_{SM}, $b^*_S(400)$ and n_S) could be found. Surprisingly using combined $b^*_{b,S}$ in stead of dividing the backscattering of particles to chlorophyllous and non-chlorophyllous part produced better results overall. Fig. 7 in paper VIII illustrates some examples of the comparison between the measured and modeled spectra. It appears that this model does not favor any water type i.e. the model does not give better results for the clear waters than e.g. for turbid waters, although the brown water case seemed to be the most difficult (Pääjärvi). The water types in this figure are from clear to very turbid starting from upper left corner. This figure shows that the model works well for other lakes than Pääjärvi (M, B) and Enäjärvi (V). All in all the results were quite varying changing from one measurement time to the next in a same lake indicating also that the measurement errors in the reflectance (Virta and Herlevi (1999)) and/or the concentrations of the optically active substances can be significant. The application of inverse modeling to interpret remote sensing data is a logical next step.

The main principle of using the inverse modeling methods is comparison of simulated spectra with measured one. It can be done in different ways: comparing spectral ratios calculated from measured and simulated spectra, using neural network or standard fitting procedures.

We compared full measured spectrum (400-750 nm; spectral resolution 2 nm in case of underwater data) with simulated ones in paper VI. All possible combinations of concentrations of optically active substances were calculated based on the ranges in concentration in our data set. A minimum value of 50% of minimal *in situ* measured concentration of each substance and a maximal value of 150% of maximum concentration were used to define simulation ranges. The best fitting spectra were selected on the basis of minimal area between the measured and modeled spectra. It was assumed that the concentrations of chlorophyll, yellow substance and total suspended matter used in modeling are close to real ones if the modeled spectrum fits with measured one.

Results of testing of the inverse model with irradiance reflectance calculated from LI-1800UW measurements are shown in Figs. 15-17. The model underestimates chlorophyll-a concentrations in the water as seen in Fig. 15. The correlation between measured and estimated values (R^2=0.80) is acceptable, but the relative errors in chlorophyll estimations are high, especially in case of small concentrations. There may be several reasons for this underestimation. Optical properties of dominating algae species in the studied lakes may have been different from those used in paper VI. There may be also problems related with methodology (described below). Absorption by yellow substance can be relatively well estimated using the model as seen in Fig. 16. Some points far from the fitted line are humic lakes or cases when measurements were carried out during cyanobacterial blooms. Optical properties, especially backscattering coefficient spectra, of cyanobacteria are very different from those used in modeling. Concentrations of non-chlorophyllous particles can be relatively well estimated (Fig. 17), but the model underestimates C_{SM} values. There is lack of data about scattering and backscattering properties of suspended matter and phytoplankton and additional investigations are needed.

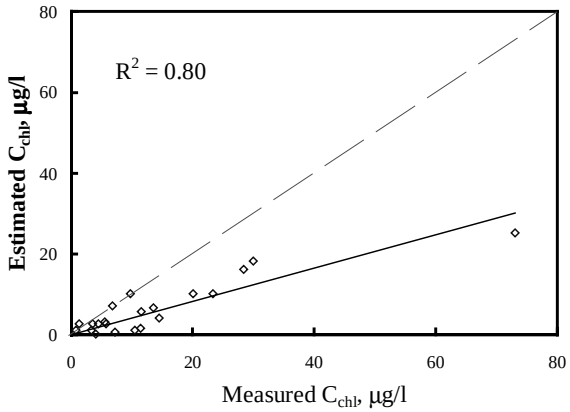

Figure. 15. Correlation between chlorophyll-a concentration measured from water samples and estimated by model simulations.

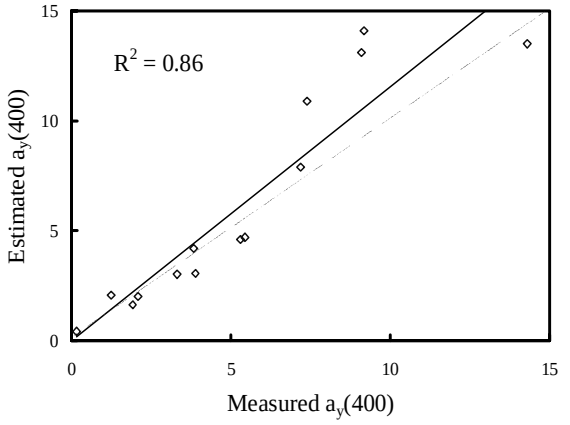

Figure 16. Correlation between yellow substance (expressed as absorption coefficient at 400 nm) concentration measured from water samples and estimated by model simulations.

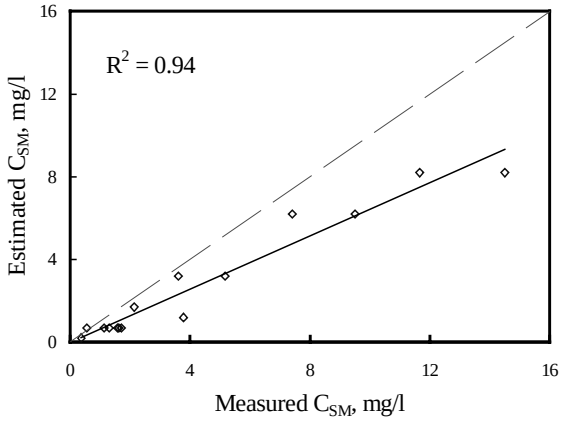

Figure 17. Correlation between concentration of suspended matter measured from water samples and estimated by model simulation.

There are some problems in inverse modeling related with the above methodology. Solutions of inverse models are not necessarily unique. Therefore the input data used must be of high quality and the information about the specific optical properties should be as extensive as possible. There may exist several combinations of the three optically active components that may give practically identical reflectance spectra. To minimize this effect our model selects ten combinations of C_{Chl}, $a_Y(400)$ and C_{SM} giving reflectance spectra most similar to the measured one. However the number of possible combinations increases very rapidly if we decrease grid steps in modeling (increasing accuracy) and even ten best fitting spectra may not give us concentrations close to the real values. The grid steps (concentration accuracy) are very important also considering computing time. Increasing accuracy we can easily increase the computation time from seconds to hours. Also to have information in the correct spectral regions could ease the problem of multiple solutions. Some of these problems could be avoided by using models to generate band ratio algorithms, which require much less computational time.

It seems however that hyperspectral modeling gives us a more universal tool for interpreting remote sensing data than using of site-specific algorithms based on spectral ratios or the like. Nevertheless, combination of these two methods is the best way in practical monitoring of inland waters using passive optical remote sensing measurements. The hyperspectral model introduced here works satisfactorily in most of the boreal waters examined, but there was large variation in its performance.

8 Conclusions

A large database from years 1994-2001 of optical properties and bio-optical parameters from Nordic waters has been collected, processed and analyzed during this study. The focus in this study was on the following subjects: variability in the optical properties in Nordic waters, relationships between inherent and apparent optical properties, spectral characteristics of optical properties (especially scattering and backscattering) and hyperspectral modeling.

- Looking at the whole data set it was seen that the variation in the optical properties is large both temporally and spatially. The variation during the summer was quite clear in some lakes. In general on the study sites there was more yellow substance and smaller particles and turbidity in May and larger scattering particles in August (chapter 7.1.).

- A representative spectrum of the attenuation coefficient, K_d for each lake was chosen to show the variability in the lakes studied here (Fig.9). The differences are distinct going from clear to turbid and brown waters. Waters can also be classified according to their K_d spectra or reflectance, R spectra (Fig.10). A relation between the broadband attenuation coefficient $K_{d,PAR}$ and the spectral attenuation coefficient $K_d(\lambda)$ was found using an analytical expression taking the value of $K_d(490)$ as a reference value.

- A model connecting spectral beam attenuation coefficient c and diffuse attenuation coefficient K_d was developed using relationships between K_d, absorption coefficient a and the scattering coefficient b for different illumination conditions. Correlation analysis of the model's results between the measured and calculated K_d gave the relationship $K_{dm} = 1.0023 K_{dc}$, with a statistically significant correlation coefficient 0.96.

- The relationships between an apparent optical property, K_d and two inherent optical properties absorption, a and scattering, b were studied. Two separate tests were used with four water type classifications in each. An initial equation in Test 1 has been found by Kirk (1984) (Eq. (36). The difference between the coefficients in the original formula and our test results was considerable, especially in the coefficient connected with scattering. One explanation given was the type of the boreal waters (brownish, but still include substantial amounts of scattering material). Another explanation may be the choice of the volume scattering function that Kirk used in his studies to find the formula. In Test 2 the situation was somewhat different. The testing equation was of the form $K_d = Aa+Bb$. The values for the coefficients A and B found by other authors were 1.0 and 0.15, respectively. Our average values were 1.21 and 0.19. Here again the value for B in brown water cases was considerably larger than the average and previous results, but was close to the original in most other cases. On the other hand the value for A was larger in almost every case and it was more stable.

- The spectral distribution of the total scattering obtained from the ac-9 data was investigated. Generally (by other authors) there seems to be evidence that b varies approximately with λ^{-1}. Our results show that the exponent of the wavelength varied between 0.13 and 2.42, the mean value being 0.78. It was also clearly larger in May/June (n_b=0.90) than in August (n_b=0.66). This can be explained by the size and type of the particles in the water. There was also in general a poor correlation between the average scattering coefficient b and the spectral wavelength dependency, except in spring (R^2=0.78 in May). However, when the correlation was good, it was positive. This was contradictory to the general results found by other authors. If one intends to find a spectrum for total scattering, the time of the year is crucial and also the type of water, but as rule of thumb b varies approximately with $\lambda^{-0.8}$ (or λ^{-1}).

- The backscattering probability, $\tilde{b}_b=b_b/b$, and the coefficient C in Eq.(16) were studied. The value of C in the Eq.(16) seemed to be changing with the water type as well as with the solar elevation and it is slightly smaller than the value proposed by *Kirk* (1984) in Eq. (17). The results of the backscattering probability study show that $\tilde{b}_b$ is growing with turbidity except in the very turbid lakes in a similar fashion with C. The size distribution and the type of scattering particles were found to be crucial also for the behavior of $\tilde{b}_b$. Moving from brown waters towards more turbid waters backscattering increases due to the increase in the amount of inorganic particles, which scatter at larger angles than organic particles. Nevertheless in very turbid cases the concentration of chlorophyll and organic particles is so large (> 40 mg m^{-3} in this study) that they dominate the scattering process where forward scattering is enhanced. The average calculated value was found to be 0.015. Our results indicate that even the 'clear' Nordic lakes contain relatively much chlorophyll to diminish the backscattering probability or the value of C. The average values for $\tilde{b}_b$ obtained from direct measurements in Sweden were found to be 0.014 in varying waters and 0.019 in lake Vänern.

- The wavelength dependence (n_B) of $\tilde{b}_b$ was studied . The average value for n_B (in λ^{-nB}) was found to be 0.63 and it was larger in spring than in autumn i.e. backscattering was more wavelength dependent (and smaller) in May than in October. Another interesting phenomenon found was: the larger the scattering (and backscattering) the smaller the wavelength dependence of $\tilde{b}_b$, which is opposite to the behavior of b seen earlier in this study.

- A hyperspectral model has been developed to test the possibility of estimating chlorophyll-a, dissolved and total organic carbon and suspended matter concentrations from the remotely measured diffuse reflectance in the turbid Nordic waters. The database for the last version of the model was collected during 1997-2001 (paper VIII). The forward model tested in paper VIII seemed to work quite well, without favoring any particular water type. The inverse mode of the model (in paper VI) worked also well, but underestimates chlorophyll-a concentrations in the water. The correlation between measured and estimated values (R^2=0.80) is acceptable, but the relative errors in chlorophyll estimations are high, especially in case of small concentrations. Absorption by yellow substance can be relatively well estimated as well as the concentrations of non-chlorophyllous particles (C_{SM}), but the model underestimates C_{SM} values

Practical Applications

The relations between the inherent and apparent optical properties are interesting from a purely physical point of view, but they have a considerable practical importance too. There are a number of practical possibilities to use these relationships described in the chapters 7.2. and 7.3.. There are maybe several reasons why one or several parameters can not be measured directly due to weather conditions, high expenses, instrument failure etc. or they are missing from time series of optical data. The relations derived above can be used to obtain representative values to replace the missing data.

1) If we have water samples and have a spectrophotometer available for measuring the beam attenuation coefficient, c, we can obtain Secchi depth values and $K_{d,PAR}$ from simple relations (chapter 7.2.1). These can be used to calculate light fields in the water column and the depth where there is enough light for photosynthesis (euphotic depth, $z_{1\%}=4.6/K_{d,PAR}$). Euphotic depth in the Finnish lakes that were investigated varies between 0.75 m in Lake Tuusulanjärvi to 6 m in Lake Päijänne. K_d values are also used in the models of primary production of biomass to calculate the PAR at any depth in water and the energy absorbed at each depth interval.
2) If we have Secchi depth data, we can calculate total beam attenuation, c and $K_{d,PAR}$ (chapter 7.2.1).
3) From $K_{d,PAR}$ values spectral K_d values can be calculated using a model described in chapter 7.2.3.
4) Measuring spectral beam attenuation coefficient $c(\lambda)$ from water samples with a relatively simple spectrophotometer, we can use a model to calculate spectral $K_d(\lambda)$ (chapter 7.2.2). The underwater solar radiation spectra may be difficult to measure in some cases, thus by our model we can estimate spatial-temporal variations of the underwater light field.
5) If we have a more advanced instrument, like ac-9, which measures both absorption and attenuation simultaneously, the inherent optical properties of a whole water column or a large area can be profiled rapidly. From this data spectra of K_d may be calculated using the relations found in this study that are suitable for Nordic waters (chapter 7.2.4).
6) Ac-9 data can be used to calculate concentrations of optically active substances (OAS), since the total absorption and scattering coefficients are additive over the constituents of the medium by the definition of inherent optical properties (Eqs. (18)-(22)).

7) We can obtain irradiance reflectance, R, or remote sensing reflectance r_D, from ac-9 data using Eq.(20), if we use the average results for $\tilde{b}_b = b_b/b$ classified into five water types.
8) We can use a hyperspectral model to deduce concentrations of OAS from remote sensing reflectance data (chapter 7.3).
    a) the model can used to monitor water quality rapidly in large areas using satellite or airborne remote sensing
    b) if a simple model is available, water quality parameters may be obtained using a portable spectrometer measuring reflectance above water on a moving boat. This is important in our small lakes and archipelago where satellite data is not usable. This kind of system could also be used in point measurements following temporal variations.
9) Spectral band ratios and empirical algorithms can be used to obtain concentrations of OAS from remote sensing reflectance. These are under development for our waters.

Future work

The relations between the diffuse attenuation coefficient, K_d to absorption, a and scattering, b are important for determination of light fields in the water. The results of this study were quite different from the earlier results by other authors and this kind of studies should be continued with large data sets to achieve more accurate relationships. A useful approach to improve the equations between K_d and a and b could be to introduce a further correction term, which could take into account the type of the water. If that would work properly then the equation could be valid for all water types. Another improvement could be to find direct relations between the coefficients A, B or C in those equations and the inherent optical properties a and b instead of classifying waters into different types (that was done here).

The spectral characteristics of scattering and backscattering probability in the water are also important for different modeling purposes and should be studied more. Some of the results found in this study were somewhat contradictory to the results found by other authors earlier. Further studies and experiments of simultaneous measurements of b_b, R, a and b should and will be performed

There is lack of data about scattering and backscattering properties of suspended matter and phytoplankton, especially from boreal waters. Studies of specific scattering properties of those substances should be performed in order to reach still more reliable remote sensing optical model results. Also specific absorption properties of phytoplankton species present in Nordic waters should be investigated more thoroughly. To the author's knowledge this kind of work is under way both in Finland and Sweden.

Acknowledgements

I found the ‘light’ (read aquatic optics) on a later stage of my scientific career almost by coincidence and find it increasingly interesting. I want to express my gratitude for Professor Matti Leppäranta and Emeritus Professor Juhani Virta for giving me a chance to start in this fascinating world of optics. They have provided the facilities at the Department of Geophysics (later Division of Geophysics) for this research and initiated the long lasting fruitful co-operation between the University of Helsinki and the Estonian Marine Institute under the framework of project SUVI (a Finnish-Estonian co-operation in optical water research).

I am truly grateful to the ‘SUVI-friends’ on the other side of the Gulf of Finland. Dr. Helgi Arst has inspired and helped me in numerous ways in optical work giving encouraging input and good ideas during our discussions as well as sharp, constructive criticism in our seminars. I want to thank Dr. Tiit Kutser and Dr. Anu Reinart as authors in many of the papers in this study for their inspiration and knowledge as experts in aquatic optics, for their help in our co-operation, for many pleasant days and hours in the numerous summer expeditions and for their friendship. I like to thank Mr. Ants Erm and Ms. Liis Sipelgas for incredible amount of work with the bio-optical measurements and for letting me use the data, for many pick-nicks on the lake shores and many hours in the boat. Without all of their help this work could not have been done.

I am most grateful to Dr. Don Pierson (Department of Limnology, University of Uppsala) for thorough and constructive criticism concerning the manuscript of this thesis and him and Dr. Niklas Strömbeck for co-operation and joint measurements and for letting me use their backscattering data.

I wish to thank Professor Timo Huttula (Division of Geophysics) also for constructive criticism concerning this manuscript and for many valuable and pleasant discussions and support during the last stages of my work.

I would like to thank Kari Kallio (Finnish Environmental Institute) for co-operation during many years, for sharing his data and for many fruitful discussions concerning optics and remote sensing.

I am grateful to Kai Rasmus, Antti Lindfors and Jens Ehn for many discussions concerning optical research, for a lot of practical help concerning instruments, data management and computers and for their ‘jokes’. I am also grateful to Riitta Lehmusjärvi, Olli Huttunen and Sirpa Rasmus (in the early stages of this work) for tedious work with data management and processing. I’d like to thank Dr. Jari Haapala for many practical advices and him and other staff at the Division of Geophysics for lunch and coffee break company.

Lammi Biological Station and Tvärminne Zoological Station (both belonging to the University of Helsinki) are acknowledged for providing excellent conditions to work and stay during the measurement campaigns.

My thanks are directed to my parents for supporting me in my search for my profession and for giving me a possibility in my youth to get interested in the aquatic sciences.

Finally and most of all I thank my wife Pauliina for love and understanding during this work and especially in the last stages for bearing the discomfort that it has brought along. I thank our two sons Tuomas and Elias for giving me lots of joy and other things to think about and do during my work.

This work was partially supported by the SUVI-project (Finnish Academy and Estonian Academy of Sciences, 1994-2001), SALMON (Satellite Lake MONitoring, Research and Development project, EU fourth Framework Program, 1997-1998) and during the last year a research project (Nr. 40010/02) by the Technology Agency of Finland.

References

Ahn, Y-H., A. Bricaud and A. Morel, 1992. Light backscattering efficiency and related properties of some phytoplankters. Deep-Sea Research, 1992; 39:1835-1855.

Arst, H. and T. Kutser, 1994. Data processing and interpretation of sea radiance factor measurements. Polar research, 13, 3-12.

Arst, H., S. Mäekivi, T. Kutser, A. Reinart, A. Blanco-Sequeiros, J. Virta and P. Nõges, 1996. Optical Investigations of Estonian and Finnish lakes. Lakes & Reservoirs: Research and Management, 2, 187-198.

Austin, R. W., 1980. Gulf of Mexico, ocean color surface truth measurements. Boundary-layer Meteorology, 18, 269-285.

Blanco, A., 1994. Underwater light field in a lake (in Finnish). Masters thesis, University of Helsinki. 1994.

Bricaud, A. and D. Stramski, 1990. Spectral absorption coefficients of living phytoplankton and non-algae biogeneous matter: A comparison between the Peru upwelling area and the Sargasso Sea. Limnol. Oceanogr., 35, 562-582.

Bricaud, A., C. Roesler and J. R. V. Zaneveld, 1995a. In situ methods for measuring the inherent optical properties of ocean waters, Limnol. Oceanogr., Vol. 40, pp. 393-410.

Bricaud, A., M. Babin, A. Morel and H. Claustre, 1995b. Variability in the chlorophyll-specific absorption coefficients of natural phytoplankton: Analysis and parameterisation, J. Geophys. Res., 100, C7, 1321-1332.

Bukata, R. P., J. H. Jerome, J. E. Burton and S. C. Jain, 1979. Determination of inherent optical properties of Lake Ontario coastal waters. Appl. Opt. 18: 3926-3932.

Bukata, R. P., J. H. Jerome, K. Y. Kondratyev and D. Pozdnyakov, 1995. Optical Properties and Remote Sensing of Inland and Coastal Waters. CRC press. New York.

Davies-Colley R. J., W. N. Vant and R. J. Wilcock, 1988. Lake water colour: comparison of direct observations with underwater spectral irradiance. Water Res. Bull., 24, 11-18.

Dekker A.G., 1993. Detection of optical water quality parameters for eutrophic waters by high resolution remote sensing. (Ph.D. thesis), Proefschrift Vrije Universiteit, Amsterdam.

Eloranta, P., 1978. Light penetration in different types of lakes in Central Finland. Holarctic Ecology 1, 362-366.

Eloranta, P., 1999. Humus and water physics. In Keskitalo, J. & Eloranta, P. (eds.). Limnology of humic waters. Backhyus Publishers, Leiden, The Netherlands, pp. 61-74, ISBN 90-5782-029-3.

Gordon, H. R., 1989. Dependence of the diffuse reflectance of natural waters on the sun angle. Limnol. Oceanogr., 35, 1484-1489.

Gordon, H. R., 1991. Absorption and scattering estimates from irradiance measurements: Monte Carlo simulations. Limnol. Oceanogr., 36, 769-777.

Gordon, H.R., O.B. Brown and M.M. Jacobs, 1975. Computed relationships between the inherent and apparent optical properties of a flat, homogenous ocean. Appl. Optics, 1975; 14:417-427.

Gordon, H.R., O.B. Brown, R.H. Evans, J.W. Brown, R.C. Smith, K.S. Baker and D.K. Clark, 1988. A semianalytical radiance model of ocean color. J. Geophys. Res., 93:10909-10924.

Gould, R. W. Jr, and R. A. Arnone, 1998. Three-dimensional modelling of inherent optical properties in a coastal environment: coupling ocean colour imagery and in situ measurements. Int. J. Remote Sensing, vol. 19, No. 11, 2141-2159.

Halturin, V. J., V.S. Suietin and S.P. Shutikov, 1983. Tables of the hydrooptical characteristics for open ocean waters, 1 (in Russian). Acad. Sci. Ukrainian SSR, Mar Hydrophys. Inst., Sevastopol, 90p.

Holmes, R.W., 1971. The Secchi disk in turbid coastal waters. Limn. Oceanogr. vol. 15, No. 5: pp. 688-694.

Horne, A. J. and C. R. Goldman, 1994. Limnology, McGraw-Hill, New York.

Højerslev, N. K., 1986. Visibility of the sea with special reference to the Secchi disc. SPIE Vol. 637 Ocean Optics VIII (1986), 294-305.

Jerlov, N. G., 1968. Optical Oceanography, Elsevier, Amsterdam.

Jerlov, N. G., 1976. Marine optics. Elsevier, Amsterdam.

Jerlov, N. G. and E. Steemann Nielsen, 1974. Optical aspects of oceanography. Academic Press. London

Jones, R.I. and L. Arvola, 1984. Light penetration and some related characteristics in small forest lakes in southern Finland. - Verh. Internat. Verein. Limnol. 22:811-816.

Kallio, K., 1999. Absorption properties of dissolved organic matter in Finish lakes. Proc. Estonian Acad. Sci. Biol. Ecol., 48:75-83.

Kallio, K., T. Kutser, S. Koponen, T. Hannonen and A. Herlevi, 1998. Estimation of water quality in Finnish lakes by an airborne spectrometer. Proceedings of V International Conference on Remote Sensing for Marine and Coastal Environments, San-Diego; Vol II:333-340.

Kallio, K., T. Kutser, and A. Herlevi, 2000. Bio-optical modeling of underwater reflectance in Finnish lakes. Proceedings of the XV Ocean Optics Conference. October 16-20, 2000, Monaco. CD-ROM. Office of Naval Research, U.S. Navy, Falls Church, VA, USA. 6 pp.

Kirk, J.T.O., 1984. Volume scattering function, average cosines, and the underwater light field. Limnol. Oceanogr. 29(2), 350-356.

Kirk, J. T. O., 1991. Dependence of relationship between inherent and apparent optical properties of water on solar altitude. Limnol. Oceanogr., 36, 455-467.

Kirk, J.T.O., 1994. Light & Photosynthesis in Aquatic Ecosystems. Cambridge University Press. Cambridge. 509 p.

Krauss, P., L. Shure and J. N. Little, 1994. Signal Processing TOOLBOX, for Use with MATLAB. The Math Works, Inc.

Kutser, T., 1997. Estimation of water quality in turbid inland and coastal waters by passive optical remote sensing. PhD Thesis. Dissertationes Geophysicales Universitatis Tartuensis 8. University of Tartu, Estonia. 69 p.

Kutser, T., H. Arst, S. Mäekivi, J-M. Leppänen and A. Blanco, 1997. Monitoring of algae blooms by optical remote sensing. In: Spiteri A editor. Remote Sensing'96, Balkema, Rotterdam 1997; pp. 161-166.

Kutser, T., H. Arst, A. Herlevi, K. Kallio and K. Eloheimo, 1998. On optical signatures of blue-green algae blooms. Proceedings of Ocean Optics XIV, Kona, Hawaii, USA, CD-ROM, 1998d.

Lee Z., K. Carder, S. Hawes, R. Steward, T. Peacock and C. Davis. Model for the interpretation of hyperspectral remote-sensing reflectance. Applied Optics, 1994, 33, 5721-5732.

Lindell, T., D. Pierson, G. Premazzi and E. Zilioli, (Eds), 1999. Manual for monitoring European lakes using remote sensing techniques. Office for Official Publications of the European Communities. Report EUR 18665. Luxembourg. pp. 125-142.

Lindfors, A. and K. Rasmus, 2000. Flow-through system for distinguishing dynamic features in the Baltic Sea. Geophysica (2000), 36 (1-2), 203-214.

Maffione, R. A., 1998. Theoretical developments on the optical properties of highly turbid waters and sea ice. Limnol. Oceanogr., 43(1), 29-33.
Maffione, R. A., and J. S. Jaffe, 1995. The average cosine due to an isotropic light source in the ocean. J. Geophys. Res. 100: 13,179-13,192.
Mobley, C. D., 1994. Light and Water. Radiative transfer in natural waters, Academic Press, San Diego, USA
Morel A., 1988. Optical modeling of the upper ocean in relation to its biogenous matter content (case I waters). J. Geophys. Res., 93, 10749-10768.
Morel, A. and L. Prieur, 1977. Analysis of variations in ocean colour. Limnol. Oceanogr. 22. 709-922.
Morel, A. and B. Gentili, 1991. Diffuse reflectance of oceanic waters: Bidirectional aspects. Appl. Optics, 32, 6864-6878.
Mäekivi, S. and H. Arst, 1996. Estimation of the concentration of yellow substance in natural waters by beam attenuation coefficient spectra. Proc. Estonian Acad. Sci., Ecology, 6:108-123.
Pegau W. S. and J. R. V. Zaneveld, 1993. Temperature-dependent absorption of water in the red and near-infrared portions of the spectrum. Limnol. Oceanogr., 38 188-192.
Phillips, D. M., and J. T. O. Kirk, 1984. Study of the spectral variation of absorption and scattering in some Australian coastal waters. Austr. J. Mar. Res. 35: 635-644.
Reinart, A., 2000. Underwater light field characteristics in different types of Estonian and Finnish lakes. PhD Thesis. Dissertationes Geophysicales Universitatis Tartuensis 11. University of Tartu, Estonia. 194 p.
Sathyendranath, S., 1986. Remote sensing of phytoplankton: a review, with special reference to picoplankton. Canadian Bulletin of Fisheries and Aquatic Sciences, 214:561-583.
Sathyendranath S., L. Prieur and A. Morel, 1989. A three component model of ocean colour and its application to remote sensing of phytoplankton pigments in coastal waters. Int. J. Remote Sensing, 10:1373-1394.
Smith, R. C., and K. S. Baker, 1981. Optical properties of the clearest natural waters (200-800 nm). Appl. Opt. 20:177-184.
Strömbeck, N., 2001. Water quality and optical properties of Swedish lakes and coastal waters in relation to remote sensing. Ph.D. thesis. Uppsala University 2001.
Vertucci F. A. and G. E. Likens, 1989. Spectral reflectance and water quality of Andirondack mountain region lakes. Limnol. Oceanogr., 34, 1656-1672.
Virta, J. and A. Herlevi, 1999. Correcting errors associated with underwater spectral irradiance measurements. Proc. Estonian Acad. Sci. Biol. Ecol., 48, 2, 143-148.
WET Labs Inc. ac-9 Users Manual. 1995. Philomath, OR. USA.
Zaneveld, J.R.V., J.C. Kitchen, A. Bricaud, and C. Moore, 1992. Analysis of in situ spectral absorption meter data, in Ocean Optics 11, Proc. SPIE 1750, pp.187-200

Notation

List of Symbols

E	irradiance defined as the radiant flux per unit area of a surface
Φ	the radiant flux
S	a surface element
$L(\theta, \varphi)$	radiance in the direction defined by zenith and azimuthal angles θ and φ
E_0	the scalar irradiance
μ	the average cosine, describes the angular distribution of underwater radiance
R	irradiance reflectance
$r_D(\lambda)$	diffuse component of remote sensing reflectance just above the water surface
K_d	diffuse attenuation coefficient for downward irradiance
$K_{d,PAR}$	broadband attenuation coefficient in the PAR region
a	absorption coefficient
b	scattering coefficient
c	beam attenuation coefficient
$\beta(\theta)$	volume scattering function as a function of scattering angle θ
$\tilde{\beta}(\theta)$	scattering phase function
L^*	path function in Eq.(10)
$\vec{E}$	net downward irradiance
K_E	attenuation coefficient of net downward irradiance
$G(\mu_0)$	coefficient determining the relative contribution of scattering to the vertical attenuation of irradiance
g_1, g_2	parameters in G
μ_0	cosine of the refracted direct solar beam just beneath the water surface
b_b	backscattering
C	a coefficient as a function of μ_0 in Eqs. (16)-(17)
λ	wavelength of radiation
S	coefficient describing the exponential slope of the yellow substance absorption curve
a^*_{ph}	specific absorption coefficient of phytoplankton
a^*_{SM}	specific absorption coefficient of non-chlorophyllous particles
a^*_y	specific absorption coefficient of yellow substance
C_y	concentration of yellow substance
C_{chl}	concentration of chlorophyll
C_{SM}	concentration of non-chlorophyllous particles
C_S	concentration of all particles
$A(\lambda)$	tabulated parameter for calculating a^*_{ph}
$B(\lambda)$	tabulated parameter for calculating a^*_{ph}
$b^*_{b,ph}$	specific backscattering coefficient of phytoplankton
$b^*_{b,SM}$	specific backscattering coefficient of non-chlorophyllous particles
Z_s	Secchi depth
$c^*(\lambda)$	attenuation coefficient measured by a spectrophotometer
τ	light transmittance
z_k	penetration depth
c_d	attenuation coefficient of distilled water
$\delta(x)$	relative variation, where x is a measured parameter
A	describing a relationship between c and b

A^*_1	influence of the particulate matter in calculations of A
F	error term due to the small-angle forward scattering in spectrophotometric measurements
$M(\lambda)$	a slope parameter in Eq. (33)
$I(\lambda)$	an intercept value in Eq. (33)
A	coefficient in equations describing relationships between K_d to a and b
B	coefficient in equations describing relationships between K_d to a and b
C	coefficient in equations describing relationships between K_d to a and b
$\tilde{b}_b=B$	backscattering probability
$\tilde{b}_{b,S}$	backscattering probability of suspended matter
n_b	exponent describing the spectral distribution of scattering coefficient
nb_b	exponent describing the spectral distribution of backscattering coefficient
n_B	exponent describing the spectral distribution of backscattering probability
n_S	exponent describing the spectral distribution of specific scattering of all particles
S_{SM}	slope of an exponential curve for absorption of suspended matter